

## RESEARCH ARTICLE

# Targeting TNF $\alpha$ produced by astrocytes expressing amyotrophic lateral sclerosis-linked mutant fused in sarcoma prevents neurodegeneration and motor dysfunction in mice

Brigid K. Jensen<sup>1,2</sup>  | Kevin J. McAvoy<sup>1,2</sup>  | Nicolette M. Heinsinger<sup>2</sup> | Angelo C. Lepore<sup>2</sup> | Hristelina Ilieva<sup>1,2</sup> | Aaron R. Haeusler<sup>1,2</sup> | Davide Trotti<sup>1,2</sup>  | Piera Pasinelli<sup>1,2</sup>

<sup>1</sup>Jefferson Weinberg ALS Center, Vickie and Jack Farber Institute for Neuroscience, Department of Neuroscience, Thomas Jefferson University, Philadelphia, Pennsylvania, USA

<sup>2</sup>Vickie and Jack Farber Institute for Neuroscience, Department of Neuroscience, Thomas Jefferson University, Philadelphia, Pennsylvania, USA

**Correspondence**

Piera Pasinelli, Jefferson Weinberg ALS Center, Vickie and Jack Farber Institute for Neuroscience, Department of Neuroscience, Thomas Jefferson University, Philadelphia, PA 19107, USA.  
Email: [piera.pasinelli@jefferson.edu](mailto:piera.pasinelli@jefferson.edu)

**Present address**

Kevin J. McAvoy, Manfredi Laboratory, Weill Cornell Medicine, Cornell University, New York, NY, USA

**Funding information**

Live Like Lou Foundation; Muscular Dystrophy Association; Family Strong 4 ALS Foundation; Farber Family Foundation; National Institutes of Health, Grant/Award Numbers: R00 NS091486, R01 NS110385, R01 NS079702, R01 NS109150, R21-NS0103118, R21 NS116761, R01 NS051488, RF1-AG057882

**Abstract**

Genetic mutations that cause amyotrophic lateral sclerosis (ALS), a progressively lethal motor neuron disease, are commonly found in ubiquitously expressed genes. In addition to direct defects within motor neurons, growing evidence suggests that dysfunction of non-neuronal cells is also an important driver of disease. Previously, we demonstrated that mutations in DNA/RNA binding protein fused in sarcoma (FUS) induce neurotoxic phenotypes in astrocytes in vitro, via activation of the NF- $\kappa$ B pathway and release of pro-inflammatory cytokine TNF $\alpha$ . Here, we developed an intraspinal cord injection model to test whether astrocyte-specific expression of ALS-causative FUS<sup>R521G</sup> variant (mtFUS) causes neuronal damage in vivo. We show that restricted expression of mtFUS in astrocytes is sufficient to induce death of spinal motor neurons leading to motor deficits through upregulation of TNF $\alpha$ . We further demonstrate that TNF $\alpha$  is a key toxic molecule as expression of mtFUS in TNF $\alpha$  knockout animals does not induce pathogenic changes. Accordingly, in mtFUS-transduced animals, administration of TNF $\alpha$  neutralizing antibodies prevents neurodegeneration and motor dysfunction. Together, these studies strengthen evidence that astrocytes contribute to disease in ALS and establish, for the first time, that FUS-ALS astrocytes induce pathogenic changes to motor neurons in vivo. Our work identifies TNF $\alpha$  as the critical driver of mtFUS-astrocytic toxicity and demonstrates therapeutic success of targeting TNF $\alpha$  to attenuate motor neuron dysfunction and death. Ultimately, through defining and subsequently targeting this toxic mechanism, we provide a viable FUS-ALS specific therapeutic strategy, which may also be applicable to sporadic ALS where FUS activity and cellular localization are frequently perturbed.

**KEYWORDS**

amyotrophic lateral sclerosis, astrocytes, fused in sarcoma, motor deficit, non-cell autonomous toxicity

This is an open access article under the terms of the [Creative Commons Attribution-NonCommercial-NoDerivs](https://creativecommons.org/licenses/by-nc-nd/4.0/) License, which permits use and distribution in any medium, provided the original work is properly cited, the use is non-commercial and no modifications or adaptations are made.

© 2022 The Authors. GLIA published by Wiley Periodicals LLC.

## 1 | INTRODUCTION

Amyotrophic lateral sclerosis (ALS) is a progressively fatal neurodegenerative disease caused by degeneration of motor neurons in the brain and spinal cord (Mulder, 1982; Strong et al., 2017). Mutations in the DNA/RNA binding protein fused in sarcoma (FUS) account for ~4% of familial ALS (fALS) and ~1% of sporadic (sALS) (Renton et al., 2014; Zou et al., 2017). Additionally, mutations in FUS are the most common genetic cause of juvenile ALS (Chen, 2021; Zou et al., 2016). Post-mortem tissues from FUS-ALS patients are marked by cytoplasmic inclusions of FUS in neurons as well as glial cells (Hewitt et al., 2010; Kobayashi et al., 2010; Kwiatkowski Jr. et al., 2009; Rademakers et al., 2010; Suzuki et al., 2012). Mislocalization of FUS has also been observed in sALS post-mortem spinal cord tissue and iPSC-derived motor neurons from sALS patients (Fujimori et al., 2018; Ikenaka et al., 2020; Tyzack et al., 2019). Strikingly, altered FUS localization is also found in both cellular and animal models of a distinct genetic form of ALS brought on by mutation of valosin-containing protein (VCP), suggesting that FUS dysregulation may more broadly contribute to disease pathogenesis than is presently recognized (Tyzack et al., 2019). Through DNA, RNA and protein-protein interactions, FUS normally functions in processes of transcription, DNA damage repair, chromosomal stabilization, RNA processing, RNA trafficking and mRNA translation (Deng et al., 2014). The most common pathogenic mutations in FUS, occurring in exons 14 and 15 near the C-terminus of the protein, disrupt nuclear import and lead to cytoplasmic mislocalization, though the degree of nuclear/cytoplasmic localization ranges widely between mutational variants as well as the cell type examined (Dormann et al., 2010; Dormann et al., 2012; Vance et al., 2009; Vance et al., 2013).

ALS pathogenesis is multifactorial, involving repercussions from defects in multiple cell types ultimately converging to damage motor neurons beyond repair (Vucic et al., 2014). While the cell-autonomous effects of FUS mutations on neuronal cells have been analyzed in several studies, considerably less is known about the effect of FUS mutations within non-neuronal cells, and how these changes lead to neuronal damage and death (Machamer et al., 2014; Scekcic-Zahirovic et al., 2017; Sharma et al., 2016; Wachter et al., 2015). Several lines of evidence suggest that astrocytes contribute to neurotoxicity in ALS. Histological studies have reported extensive reactive astrogliosis, gross astrocytic abnormalities, and the presence of protein aggregates, inclusion bodies, and RNA foci in astrocytes within disease-affected areas of patients and animal models of ALS (Averback, 1986; Buijn et al., 1997; Conlon et al., 2016; Gong et al., 2000; Kamo et al., 1987; Kimura & Budka, 1984; Kushner et al., 1991; Mizielinska et al., 2013; Murayama et al., 1991; Nagy et al., 1994; Popova & Sakharova, 1982). A myriad of molecular changes have also been reported in astrocytes from both ALS patient tissues and animal models (Filipi et al., 2020; Rostalski et al., 2019; Valori et al., 2014). Notably, aberrant transcription factor activity (NF- $\kappa$ B, c-jun, JNK, and STAT3), increased inflammatory gene transcripts, and increased cytokine production have been described (Dokalis & Prinz, 2018; Gandelman et al., 2010; Hensley et al., 2003; Migheli et al., 1997; Phatnani et al., 2013; Tong

et al., 2013; Tripathi et al., 2017; Tyzack et al., 2017; Wang et al., 2011). Finally, primary astrocytes from transgenic mice carrying ALS-causative gene mutations, primary rodent astrocytes transduced with mutant ALS genes, and astrocytes derived from patient induced pluripotent stem cells have all been found to reduce the viability of wild-type motor neurons (Di Giorgio et al., 2007; Meyer et al., 2014; Nagai et al., 2007; Qian et al., 2017). These studies provide compelling evidence that astrocytes could be a valuable therapeutic target in ALS. However, significant gaps in knowledge currently exist in our understanding of astrocytes as mediators of ALS pathogenesis.

We hypothesized that mutations in FUS could also cause dysregulation of astrocytes, particularly as FUS expression is ubiquitous in the nervous system and FUS participates broadly in essential gene expression regulation processes. Previous studies demonstrate that FUS silencing in rodent astrocytes leads to differential expression of >2000 genes in vitro (Fujioka et al., 2013), while CNS silencing of FUS in marmosets induces activation and proliferation of astrocytes absent of any gross neuronal pathology (Endo et al., 2018). Conversely, overexpression of wild-type FUS has been shown to substantially alter the inflammatory profile of mouse and human astrocytes in vitro (Ajmone-Cat et al., 2019). Mouse models of FUS also indicate the involvement of non-neuronal cells in disease. Mice harboring the FUS<sup>P525L</sup> mutation with ubiquitous expression display accelerated disease progression compared with motor-neuron restricted expression (Sharma et al., 2016). In the well-characterized FUS<sup>ANLS</sup> mouse model, excision of mutant FUS specifically from motor neurons was found to delay, but not prevent motor deficits, suggesting that non-cell autonomous effects could be sufficient to drive motor dysfunction (Scekcic-Zahirovic et al., 2017). However, it is important to note that the specific contribution of astrocytes to disease course in these models is undetermined. Intriguingly, rare cases of cortical neurodegeneration associated with astrocyte-predominant tauopathy have been linked to a novel FUS variant, however, the pathogenicity of this variant is still uncertain (Ferrer et al., 2015). Taken together, these studies indicate that further examination of the effects of FUS dysregulation in astrocytes is warranted (Scekcic-Zahirovic et al., 2017).

Previously, we demonstrated that astrocytes expressing human ALS-linked FUS mutations are toxic to wild-type spinal motor neurons in vitro (Kia et al., 2018). We observed that when expressed in astrocytes, mutant FUS induces activation of the transcription factor NF- $\kappa$ B, resulting in elevated production of pro-inflammatory cytokine TNF $\alpha$  (Kia et al., 2018; Qosa et al., 2016). Following binding to receptors on motor neurons, we noted TNF $\alpha$ -induced changes to motor neuron AMPA receptors, which caused sensitization to excitotoxic cell-death (Kia et al., 2018).

To follow up on those studies, here we explored whether mutant FUS expression in astrocytes in vivo is also sufficient to induce motor neuron dysfunction and degeneration. We have generated an acute FUS-ALS-astrocyte model in adult mice, using AAV9 to deliver astrocyte-specific promoter (*gfa<sub>104</sub>*) driven GFP-tagged human FUS. The *gfa<sub>104</sub>-eGFP*, as reference, or *gfa<sub>104</sub>-eGFP:hFUS<sup>R521G</sup>* (mtFUS) constructs were introduced into the cervical spinal cord of p180 mice by intraspinal injection. The hFUS<sup>R521G</sup> mutation is a well-established

hFUS variant known to cause ALS, localized to the C-terminal PY-NLS (nuclear localization sequence) region of the protein (Dormann & Haass, 2011). It is also one of the variants that we previously utilized in our *in vitro* studies exploring non-cell autonomous effects of astrocyte-expressed mtFUS (Kia et al., 2018; Qosa et al., 2016). We demonstrate that specific expression of hFUS<sup>R521G</sup> in astrocytes causes upregulation of TNF $\alpha$ , reduction in grip strength and wirehang endurance motor functions, and ultimately a loss of spinal motor neurons. These effects were not seen when TNF $\alpha$  knockout animals underwent the same procedure. We next tested whether FUS-mediated effects could be attenuated through prevention of TNF $\alpha$  signaling in wildtype animals. AAV9 eGFP:hFUS<sup>R521</sup> intraspinal injections were performed with or without concomitant TNF $\alpha$ -neutralizing antibody (anti-TNF $\alpha$ ,  $\alpha$ -TNF $\alpha$ ). In animals receiving  $\alpha$ -TNF $\alpha$ , we observed significant rescue of grip strength performance and preservation of motor neurons. Finally, we designed a protocol which allowed for eGFP:hFUS<sup>R521</sup> to be expressed for 1 week prior to administration of TNF $\alpha$ -neutralizing antibody. In these animals, grip strength and motor neurons were preserved at 2-weeks following  $\alpha$ -TNF $\alpha$  addition. However, when evaluation of this model was performed at 2-months post-therapeutic administration, the efficacy of this intervention was decreased, with both grip strength performance and motor neuron numbers being significantly reduced.

Overall, these studies further substantiate that astrocytes contribute to disease in genetic models of ALS. We provide novel findings that astrocytic expression of FUS is sufficient to induce pathogenic changes *in vivo* through activation of the NF- $\kappa$ B and TNF $\alpha$  pathway. We demonstrate that TNF $\alpha$  is the critical driver of astrocyte-mediated motor neuron toxicity in our model, as TNF $\alpha$  knockout animals expressing mtFUS retain functional motor behavior and motor neuron numbers. Notably, we also provide evidence that therapeutics designed to diminish activation of the TNF $\alpha$  pathway may be effective in reducing motor neuron degeneration in FUS-ALS.

## 2 | MATERIALS AND METHODS

### 2.1 | Antibodies

Abcam: anti-FUS (Abcam Cat# 84078, RRID:AB\_2105201, 1:1000), anti-GFP (Abcam Cat# ab13970, RRID:AB\_300798, 1:1000); Cell Signaling: anti-NeuN (Cell Signaling Cat# 24307, RRID:AB\_2651140, 1:400); Millipore: anti-ChAT (Millipore RRID:AB\_2079751, 1:1000), anti-GFAP (Millipore Cat# AB5541, RRID:AB\_177521, 1:500), anti-Olig2 (Millipore, RRID: AB\_9610, 1:1000); Sigma: anti-MMP9 (Sigma-Aldrich Cat# M9570, RRID:AB\_1079397, 1:60); Wako: anti-Iba1 (Wako Cat# 019-19,741, RRID:AB\_839504, 1:1000).

### 2.2 | Other reagents

Agilent: Dako target antigen retrieval solution; AmericanBio: non-fat dry milk omniblock; Bio-Rad Laboratories: 4%–20% Mini-PROTEAN

TGX stain-free gel, broad-spectrum molecular weight ladder, Tris/glycine running buffer, Tris/glycine transfer buffer; Decon Laboratories: 200-proof ethanol; Electron Microscopy Sciences: 16% paraformaldehyde, Citifluor AF3; Millipore Sigma:  $\beta$ -mercaptoethanol, bovine serum albumin (BSA), Bradford reagent, deoxycholic acid, dithiothreitol (DTT), (ethylenedinitrilo) tetraacetic acid (EDTA), GeneRuler 1 kb Plus, HEPES, hydrogen peroxide, immobilon-FL membranes, magnesium chloride hexahydrate (MgCl<sub>2</sub>), sodium dodecyl sulfate, sodium hydroxide; National Diagnostics: Histoclear; Research Products International: DEPC H<sub>2</sub>O; ThermoFisher: agarose, Hoechst 33258 pentahydrate (bis-benzimide), methanol, normal goat serum, phosphate-buffered saline (PBS), potassium chloride, protease inhibitors, sodium chloride, Tris-HCl, Tween-20; US Biological: Nonidet (NP-40).

### 2.3 | Animals

Adult p180 female non-transgenic C57BL/6J mice were acquired from Jackson Laboratories (<https://www.jax.org/strain/000664>) and housed in a humidity-, temperature-, and light-controlled animal facility with *ad libitum* access to standard chow and water. For experiments involving TNF $\alpha$  knockout animals, the following genotype was also acquired from Jackson Laboratories:

B6.129S-Tnf tm1Gkl/J (<https://www.jax.org/strain/003008>). Homozygous female mice of this line were obtained at 12-weeks of age, which have a targeted deletion of the TNF $\alpha$  gene by replacement of 40 base pairs of the 5' UTR, the ATG start codon, and the entire coding region for the first exon and part of the first intron with the MC1neopA cassette (Pasparakis et al., 1996). A 12-week-old female wildtype non-transgenic C57BL/6J mice as indicated above were acquired at the same time to serve as cohort controls, as the transgenic animals were also inbred using this background. Knockout and wildtype animals were aged to p180 in-house prior to intraspinal injection surgeries, to age-match timing with other surgical paradigms. In all studies described herein, female mice were used to better control for variances in animal starting weight and weight throughout the course of experimentation.

In total, this study represents the usage of 167 animals which underwent surgery, including animals for optimization of surgical techniques and viral delivery/dosing. For each experimental cohort, power analysis was performed to ensure adequate animals were represented per group for appropriate statistical comparisons based on an anticipated moderate effect size. Specific animal numbers used for evaluation of each experimental parameter can be found explicitly within all figure legends. To minimize animal numbers, based on methods involved, the same animals could frequently be used for multiple assays, such as motor behavior assessment, immunostaining, and mRNA analysis.

All experimental procedures were approved by the Thomas Jefferson University Institutional Animal Care and Use Committee (IACUC) and conducted in compliance with the National Institutes of Health Guide for the Care and Use of Laboratory Animals.

## 2.4 | Virus production

AAV9 vectors were generated by the University of Pennsylvania Penn vector core using a plasmid designed as follows. The  $gfa_{104}$  promoter element was from the pAAV.GFA104.PI.eGFP.WPRE.bgH plasmid, which was a gift from Philip Haydon (Addgene plasmid #100896). AAV9  $gfa_{104}$ -eGFP::hFUS<sup>R521G</sup> vectors were created by subcloning with a plasmid containing N-terminally eGFP tagged human R521G (CGC to GGC) FUS in a pcDNA3.1/nV5-DEST backbone (Kia et al., 2018).

## 2.5 | Intraspinal delivery of AAV9 virus

Intraspinal delivery of AAV9 in p180 mice was carried out as previously described (Li et al., 2014; Li et al., 2015). Briefly, deeply anesthetized mice underwent incision of their dorsal skin and underlying muscle, with retraction so that the spinous processes between C2 and T1 were visible. Bilateral laminectomy at spinal levels C4, C5, and C6 was then followed by six total injections, each containing a  $1 \times 10^{11}$  GC/injection of the AAV- $gfa_{104}$ -eGFP viruses in  $1 \mu\text{L}$  total volume using a Hamilton gas-tight syringe mounted on an electronic UMP3 micropump (World Precision International, Sarasota FL). A 33-gauge  $45^\circ$  beveled needle was lowered 0.8 mm below the dorsal surface of the spinal cord to target the ventral horns. Targeting of injections were guided along the lateral axis corresponding to the middle of each spinal segment, and along the rostral-caudal axis at the location of dorsal root entry for each bilateral injection set at levels C4, C5, and C6. Each injection was delivered over a 5-min interval at a constant rate. For all experiments, sham surgery control animals underwent identical surgical procedures and laminectomies, as well as needle placement and insertion. Instead of  $1 \mu\text{L}$  total AAV- $gfa_{104}$ -eGFP virus injection to each location, a PBS filled Hamilton syringe was used and the micropump was not initiated. Following completion of surgical procedures, overlying muscles were then closed in layers with sterile 4-0 silk sutures. The skin incision was closed using sutures followed by sterile wound clips. Animals recovered on a heating pad until awake and then were returned to their home cages. To minimize pain and discomfort, animals were administered subcutaneous sterile saline fluids, buprenorphine analgesic at 0.05 mg/kg, and cefazolin antibiotic at 10 mg/kg at the time of surgery, and at 12-h intervals for 24 h following surgery. Initially, animals were monitored daily for the first 2 weeks following surgery. In two month cohort animals, following this 2 week mark, monitoring occurred every 3 days until the conclusion of the study. Animals were checked for signs of distress and/or pain, as well as ambulatory potential and ability to feed/water themselves.

## 2.6 | Intraspinal delivery of anti-TNF $\alpha$ antibody

Our previous in vitro experiments demonstrated efficacy of targeting astrocytic-derived TNF $\alpha$  to prevent motor neuron toxicity using a TNF $\alpha$  neutralizing antibody (Kia et al., 2018). In the present study,

functional grade anti-TNF $\alpha$  ( $\alpha$ -TNF $\alpha$ , MP6-XT22, ThermoFisher) antibody was used. In our first therapeutic paradigm, antibody was co-injected with AAV at the time of surgeries, at the previously demonstrated effective dosing of 2 mg/kg, while maintaining the same  $1 \mu\text{L}$  total injection volume and viral titer. This antibody has been previously shown in rodent models to be safe, effective, and well-tolerated at this dosing (Finsterbusch et al., 2016; Via et al., 2001). Assessment of motor behavior and motor neuron numbers were carried out 2 weeks following surgery to determine potential beneficial effects of this therapeutic intervention.

In our second therapeutic paradigm, intraspinal delivery of AAV9 Virus was performed as indicated, with a non-adhering dressing (Adaptic non-adhering dressing by Systagenix) applied over the spinal cord prior to surgical closure. Following 1 week of viral expression, animals were again deeply anesthetized, their original surgical incision re-opened, and the spinal cord was again exposed by retraction of dorsal skin and underlying muscle. The non-adhering dressing was gently removed to re-expose the spinal cord. A pre-saturated gelfoam sponge (Gelfoam Dental sponges from Pharmacia & Upjohn Company) was directly applied to the exposed spinal cord region. Animals in this grouping either received gelfoam that had been saturated with functional grade anti-TNF $\alpha$  antibody at the 2 mg/kg dosing, with sterile saline solution making up the remaining liquid volume, or a sterile saline saturated gelfoam as a control. Following completion of this second surgical procedure, overlying muscles were again closed with sterile 4-0 silk sutures. The skin incision was closed using sutures followed by sterile wound clips. Animals recovered on a heating pad until awake and then were returned to their home cages. To minimize pain and discomfort, animals were administered subcutaneous sterile saline fluids, buprenorphine analgesic at 0.05 mg/kg, and cefazolin antibiotic at 10 mg/kg at the time of surgery, and at 12-h intervals for 24 h following surgery. Assessment of motor behavior, and motor neuron numbers were carried out 2 weeks and 2 months following surgery to determine potential beneficial effects and longevity of this therapeutic intervention.

Animals receiving TNF $\alpha$  neutralizing antibody were checked for signs of distress and/or pain, as well as ambulatory potential and ability to feed/water themselves as indicated in the virus only cohorts above. Additionally, these animals were closely monitored to detect any adverse effects that local application of the antibody may have caused. At the dosing referred by previous studies and instituted here, no negative adverse effects were documented upon use of this antibody.

## 2.7 | Motor behavioral assessments

Wirehang latency to fall was measured by placing mice upside down on a metal wire grid at a height of 50 cm above a soft landing pad. The amount of time spent hanging onto the cage prior to falling was measured, with a maximum cutoff of 120 s. Muscle grip strength was determined for combined forelimbs using a DFIS-2 Series Digital Force Gauge (Columbus Instruments). Grip strength testing was performed by allowing the mice to grasp a thin "Y" bar attached to the

**TABLE 1** Primer pairs used for qPCR analysis of mouse spinal cord tissue samples

| Gene         | Forward               | Reverse               |
|--------------|-----------------------|-----------------------|
| eGFP         | TCAAGATCCGCCACAACATC  | GTGCTCAGGTAGTGGTTGTC  |
| GAPDH        | AACAGCAACTCCCACTCTTC  | CCTGTTGCTGTAGCCGTATT  |
| GFAP         | AGAAAGGTTGAATCGCTGGA  | CGGCGATAGTCGTTAGCTTC  |
| hFUS         | GACCGTGGTGGCTTCAATAA  | CCTTGACAAAAGATGGTGTG  |
| msFUS        | CAGCAGCAAAGTTCACAATC  | CTCTGAGAACTGCCACCATAA |
| TNF $\alpha$ | CTGAGTTCTGCAAAGGGAGAG | CCTCAGGGAAGAATCTGGAAG |

**TABLE 2** Solutions used to extract DNA for PCR analysis

| 10 $\times$ solution A      | 10 $\times$ solution B      |
|-----------------------------|-----------------------------|
| 0.5 g NaOH                  | 3.15 g Tris HCl             |
| 0.037 g EDTA                | 50 ml DEPC H <sub>2</sub> O |
| 50 ml DEPC H <sub>2</sub> O |                             |

Note: Dilute both to 1 $\times$  Solutions before use by adding 5 ml 10 $\times$  to 45 ml DEPC H<sub>2</sub>O.

force gauge. This was followed by pulling the animal away from the gauge until the forelimbs simultaneously released the bar. Force measurements were averaged from five trials for each animal.

## 2.8 | Spinal cord preparation for immunofluorescence and qPCR

Mice were euthanized by carbon dioxide asphyxiation and whole animals were fixed using standard procedures. Briefly, a perfusion needle connected to a peristaltic pump was placed in the posterior end of the left ventricle of the heart. Mice were first perfused with approximately 200 ml phosphate buffered saline followed by 200 ml of 4% paraformaldehyde. Whole spinal cords were dissected and placed in 4% paraformaldehyde at 4°C for 30 min, then moved to 2% paraformaldehyde overnight. Paraformaldehyde was rinsed off the tissue with three consecutive washes with a 1:1 solution of potassium monosulfate and potassium bisulfate buffer. Spinal cords were then placed in 30% sucrose for 24–48 h until tissue sinking. Following anatomical assessment, cervical spinal cord regions were frozen into Tissue-Tek OCT solution and sectioned at 30  $\mu$ m using a cryostat (Thermo Scientific) and placed onto charged glass slides.

For tissue immunofluorescence, blocking, permeabilization, and staining conditions were carried out according to standard protocols and based on the manufacturer instructions for each antibody. Slides containing 30  $\mu$ m cervical spinal cord tissue sections were heated overnight at 55°C, followed by Histoclear and rehydration in sequential 100%, 95%, 90%, and 70% ethanol washes. Incubation in hydrogen peroxide (3% in methanol) for 30 min was used to block endogenous peroxidase activity. Unmasking of antigens was achieved by incubation in target antigen retrieval citrate solution for 1 h at 95°C. Sections were next blocked in normal goat serum (10% in PBS) for 1 h at room temperature (5% BSA instead of goat serum for ChAT)

and incubated in primary antibodies overnight at 4°C (48 h incubation specifically for ChAT). Primary antibodies included: anti-ChAT (Millipore RRID:AB\_2079751, 1:1000), anti-FUS (Abcam Cat# 84078, RRID:AB\_2105201, 1:1000), anti-GFAP (Millipore Cat# AB5541, RRID:AB\_177521, 1:500), anti-GFP (Abcam Cat# ab13970, RRID:AB\_300798, 1:1000), anti-MMP9 (Sigma-Aldrich Cat# M9570, RRID:AB\_1079397, 1:60), anti-NeuN (Cell Signaling Cat# 24307, RRID:AB\_2651140, 1:400), anti-Iba1 (Wako Cat# 019-19,741, RRID:AB\_839504, 1:1000), and anti-Olig2 (Millipore, RRID: AB\_9610, 1:1000). Following PBS washing, secondary labeling with AlexaFluor488, AlexaFluor594, or AlexaFluor647 (Life Technologies) were used to enable visualization. Hoechst stain (ThermoFisher) was used to label nuclei. Stained slides were mounted in Citifluor AF3 (Electron Microscopy Sciences). Image capture and processing were accomplished using a Nikon A1+ confocal microscope with NIS-Elements software. ChAT<sup>+</sup> and MMP<sup>+</sup> cells were assessed using bilateral ventral horn images with manual counting.

For qPCR analysis, RNA was isolated from fixed spinal cord sections using the PureLink RNA Mini Kit (ThermoFisher), reverse transcribed using the QuantiTect Reverse Transcription Kit (Qiagen), prepared for qPCR using a SYBR Green qPCR master mix (ThermoFisher) and analyzed on QuantStudio 5 Real-Time PCR System (ThermoFisher). Samples were measured in triplicate from each animal for each gene of interest. Data were normalized using GAPDH levels, fold change between groups is represented. Primer pairs obtained from Integrated DNA Technologies (Coralville, IA) for each gene are given in Table 1.

## 2.9 | Spinal cord preparation for ELISA and Western blotting

Mice were euthanized by carbon dioxide asphyxiation. Cervical spinal cords were then dissected, and flash frozen in liquid nitrogen. Dissociated single-cell suspensions were prepared using homogenization buffer containing: 10 mM HEPES pH 7.9, 1.5 mM MgCl<sub>2</sub>, 10 mM KCl, 0.5 mM DTT, and protease inhibitor cocktail (1:100), and then underwent centrifugation at 845 g at 4°C for 5 min.

## 2.10 | TNF $\alpha$ ELISA

The supernatant from this homogenization step was used to evaluate levels of TNF $\alpha$  using the mouse TNF alpha high sensitivity ELISA Kit

**TABLE 3** Primer pairs used for PCR analysis of wildtype and TNF $\alpha$  knockout animals

|                         | Forward              | Reverse               |
|-------------------------|----------------------|-----------------------|
| Genotyping control (ms) | CGTTCGGATAATGTGAGACC | TTCGAATAATGTGTGTTAGCC |
| TNF $\alpha$            | TAGCCAGGAGGGAGAACAGA |                       |
| TNF $\alpha$ wildtype   |                      | AGTGCCTCTTCTGCCAGTTC  |
| TNF $\alpha$ knockout   |                      | CGTTGGCTACCCGTGATATT  |

according to manufacturer's instructions (Invitrogen, BMS607HS). Briefly, microwell strips pre-coated with anti-TNF $\alpha$  capture antibody were washed with wash buffer. Samples and standards were added to wells along with biotin-conjugate and allowed to incubate for 2 h. Wells were washed and then incubated with streptavidin-HRP for 1 h. Following another round of washing, wells were incubated next with amplification solution I for 15 min, were washed again, and then incubated with amplification solution II for 30 min. After a final washing step, wells were incubated with a TMB substrate solution for 15 min. All incubations were performed with shaking at room temperature. The Stop Solution was added immediately prior to plate reading. The color intensity of each well was measured at 450 nm using a Cytation5 microplate reader (Biotek).

## 2.11 | Western blotting

From each animal, dissociated cells were then resuspended in RIPA buffer containing: 150 mM NaCl, 1% Nonidet (NP-40), 0.5% deoxycholic acid, 0.1% sodium dodecyl sulfate, 50 mM Tris-HCl, 2 mM EDTA, and protease inhibitor cocktail (1:100). These suspensions were pulse-sonicated 3 times for 10 s each with 2 min rest on ice between rounds, and spun at 21,130 g at 4°C for 30 min. The Bradford method was used to determine protein concentrations of supernatant fractions. A 25  $\mu$ g of protein was loaded onto a Mini-PROTEAN TGX stain-free gel (4%–20%) for electrophoretic separation, along with a molecular weight ladder. Following separation, total protein levels were determined by imaging with the pre-set stain-free gel parameters on the Bio-Rad ChemiDoc Touch Imaging System. Proteins were transferred onto Millipore Immobilon-FL membranes and were blocked in PBST (PBS + 0.1% Tween-20) and milk (5%) for 30 min at room temperature prior to overnight incubation at 4°C with primary antibodies in PBST +5% milk. Primary antibodies used were: anti-FUS (Abcam Cat# 84078, RRID:AB\_2105201, 1:1000), and anti-GFP (Abcam Cat# ab13970, RRID:AB\_300798, 1:1000). Three PBST washes were followed by incubation with LiCor antigen species-specific fluorescent probe-conjugated secondary antibodies (1:15,000 dilution in PBST +5% milk) for 1 h at room temperature. An Odyssey Infrared Imaging system (LiCor) equipped with ImageStudio was used for membrane visualization. Bands of interest were selected at the heights corresponding to the molecular weight of the protein of interest using ImageJ software. Pixel intensities of these defined areas were normalized to a horizontal section of the Bio-Rad total protein image spanning a broad molecular weight range. As such, overall intensity of each lane was determined to account for variability in tissue lysate extracts.

## 2.12 | PCR analysis of TNF $\alpha$ knockout animals

Ear snips were collected at the time of mouse euthanasia for the TNF KO and wildtype paired experiments. DNA was isolated from these samples as follows. A 75  $\mu$ l of 1 $\times$  Solution A was added to tissues, which were then heated to 95°C for 30 min and then cooled to 4°C. After mixing, 75  $\mu$ l of 1 $\times$  Solution B was added and mixed. Ingredients for solutions found in Table 2.

Genotyping was performed using the suggested primer pairs provided by the Jackson Laboratory for these animals (below), along with the associated recommended PCR cycling times and temperatures (<https://www.jax.org/Protocol?stockNumber=003008&protocolID=22433>). PCR results were run on a 1.5% agarose gel, along with a DNA ladder (GeneRuler 1 kb plus). Primer pairs obtained from Integrated DNA Technologies (Coralville, IA) are given in Table 3.

## 2.13 | Data analysis considerations

Throughout this study, animals were numbered according to surgery order, and were randomized into genotype and treatment groups. Grip strength and wirehang latency to fall behavioral analysis were evaluated with the individual performing the test blinded to the animal cohorts. Similarly, imaging and counting of motor neuron immunofluorescence staining was performed in a blinded manner.

## 2.14 | Statistical analysis

Prism 8.0 Software (GraphPad) was used to perform all statistical analyses. Statistical significance for pairwise assessment in experiments with multiple groups was accomplished using One-way ANOVA with post hoc Dunnett's multiple comparison test or Sidak's multiple comparison test where applicable. Student's *t* test was used to evaluate any direct comparison of only two groups. All data are expressed as mean  $\pm$  SEM, with values of *p* < .05 considered significant.

## 3 | RESULTS

### 3.1 | Generation and characterization of an acute in vivo mouse model for effects of mutant FUS expression in astrocytes

We generated AAV9 encoding either eGFP alone or hFUS<sup>R521G</sup> fused at the N-terminus to eGFP (eGFP:hFUS<sup>R521G</sup>, hereafter

referred to as mtFUS) placed under control of the minimal GFAP promoter element  $gfa_{104}$ . We performed six injections, bi-laterally, containing  $1 \times 10^{11}$  GC/injection eGFP or mtFUS virus across the C4-C6 region of the spinal cord of p180 mice (Figure 1a). We observed high efficiency of AAV9 delivery and enriched targeting to the ventral horn through the intraspinal delivery method using

either our eGFP or mtFUS viruses (Figure 1b). We quantified the transduction efficiency of these vectors by counting eGFP positive cells as a percentage of total cells using nuclear marker DAPI, after 7 days post-injection (DPI) and found  $12.7\% \pm 5.1\%$  of total spinal cord cells transduced (Figure S1a). In further evaluating only cells within the targeted ventral horn region,  $37.8\% \pm 8.7\%$  transduction

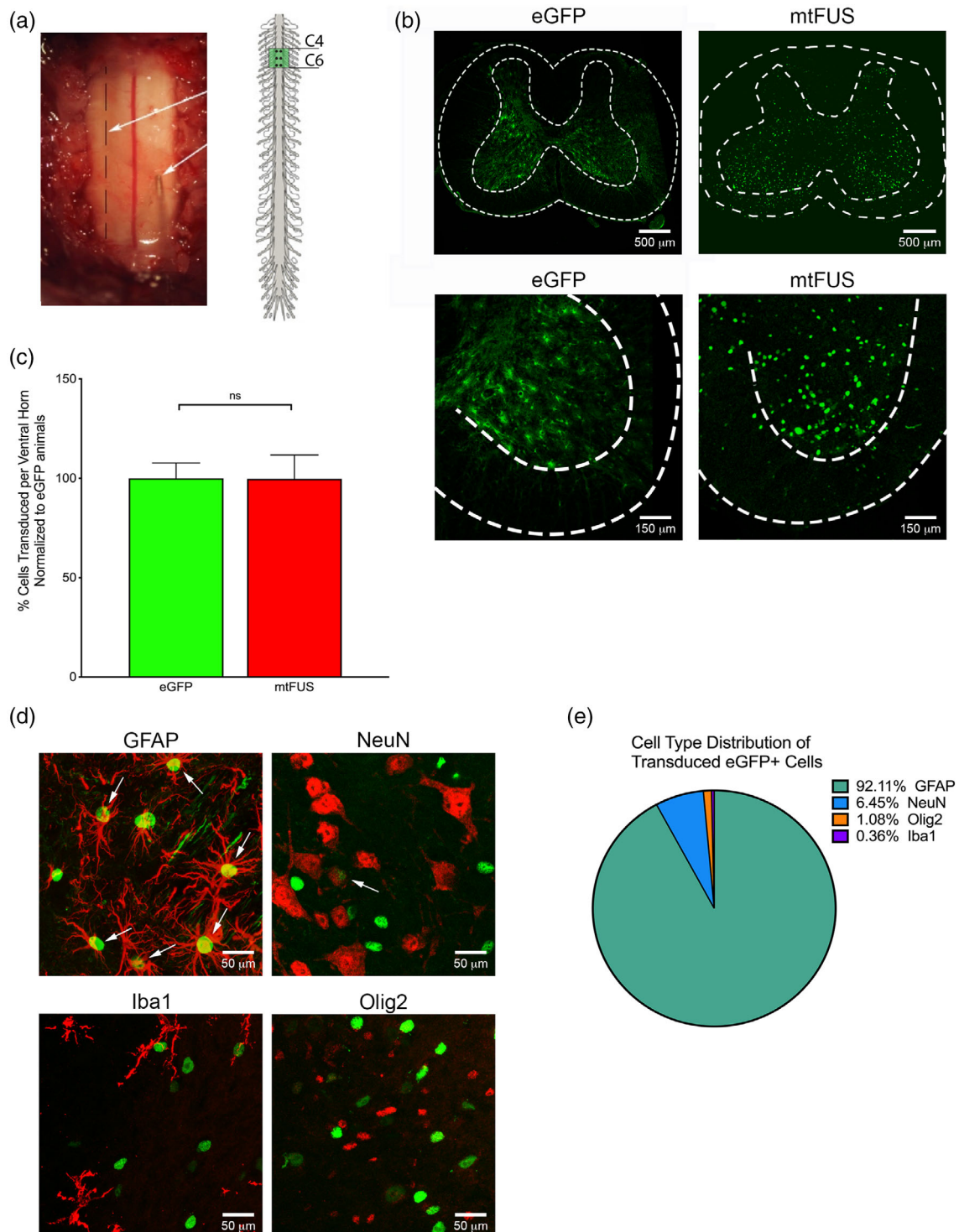


FIGURE 1 Legend on next page.

efficiency was observed (Figure S1a). Direct comparison of the percentage of cells transduced per ventral horn revealed equal transduction efficiencies between our eGFP and mtFUS viruses (Figure 1c). We also characterized the efficiency of AAV9-GFA104 to transduce astrocytes, by staining spinal cord sections with various cell-type markers at 7 DPI. We analyzed the overlap of eGFP signal with markers for astrocytes (GFAP), neurons (NeuN), microglia (Iba1) and oligodendrocytes (Olig2) (Figure 1d). Quantification of this analysis revealed that the cell lineages represented by eGFP<sup>+</sup> neurons were: 92.11% astrocytes, 6.45% neurons, 1.08% oligodendrocytes, and 0.36% microglia (Figure 1e). These data demonstrate that intraspinal delivery of AAV9-gfa<sub>104</sub> robustly transduces astrocytes with minimal leakage into the other cell populations. In evaluating mtFUS localization of transduced cells, we frequently observed a strong nuclear signal along with aggregated cytosolic puncta (Figure S1b). Before analyzing potential mtFUS-mediated effects, to better characterize this model, we assessed expression of eGFP and mtFUS over time. No differences in overall body weight were observed following an 8-week observation period post-surgery (Figure S1c). Robust eGFP expression was observed in as little as 3 days in both eGFP and mtFUS animals when evaluated by immunofluorescent staining (Figure S2a). At 14 days post-injection, eGFP levels were still robustly and significantly expressed in both eGFP and mtFUS cohort groups when evaluated by immunofluorescent staining of spinal cords, qRT-PCR mRNA analysis, and western blotting for eGFP protein (Figure S2a–c). Evaluation of FUS levels in these mice revealed similar levels of total FUS protein when evaluated by immunofluorescence and western blotting (Figure S2d–f). Of note, in qRT-PCR analysis, only mtFUS animals showed mRNA specific to the human FUS sequence ( $p < .01$ ) (Figure S2e). Similarly, only mtFUS animals had a second FUS band on the western blot corresponding to the eGFP-FUS fusion protein (Figure S2f). As a result of these assessments, we concluded that this model was appropriate for studying the potential effects of astrocytic mtFUS expression in vivo.

### 3.2 | Motor deficits and loss of motor neurons occur when mtFUS is expressed in astrocytes

An advantage of utilizing intraspinal injection sites spanning the C4–C6 region of the mouse spinal cord is that motor neuron loss in this region has the potential to impact readily measurable forelimb motor behaviors (Bacskaï et al., 2013). Assessment of these behaviors enabled a first-pass evaluation of whether mtFUS expression in astrocytes in vivo produced motor deficits over time. At 14 days post-injection, we noticed overt weakness of the mouse forelimb in mtFUS expressing animals, but not eGFP alone. We measured a permanent reduction in both grip strength and wire hang endurance, beginning at 2 weeks, in mtFUS animals but not eGFP-alone (Figure 2a–b). At 2 weeks, mtFUS animals showed a wire hang latency of  $30.83 \pm 6.9$  s, compared with eGFP animals who had a wire hang latency of  $81.7 \pm 13.4$  s ( $p < .01$ ). Similarly, at 2 months this phenotype was maintained, with mtFUS animals having a wire hang endurance of  $23.4 \pm 7.8$  s, compared with eGFP animals with a wire hang latency of  $91.7 \pm 8.9$  s ( $p < .0001$ ) (Figure 2a). As a second behavioral measure, grip strength was also assayed at these timepoints. At 2 weeks mtFUS animals had a grip strength of 0.10 kg compared with eGFP animals with a grip strength of 0.16 kg ( $p < .01$ ), and at 2 months mtFUS animals had a grip strength of 0.08 kg compared with the 0.18 kg grip strength of eGFP controls ( $p < .001$ ) (Figure 2b). Assessment of motor behavior over time was also evaluated, by directly comparing the wire hang latency to fall and grip strength force of individual animals at these two timepoints. eGFP animals which had higher baseline performance at 2 weeks all improved in both measures when reassessed at 2 months. In contrast, the mtFUS animals which had significant deficits already at 2 weeks, continued to all decline in performance when assessed by either motor task (Figure 2c,d).

We next sought to determine whether this loss of motor function correlated with a loss of motor neurons. We counted motor neurons in spinal cord sections from these mice using two motor neuron markers: matrix metalloproteinase 9 (MMP9), which is a specific marker for the large motor neuron pool most vulnerable in ALS, and

**FIGURE 1** Generation and characterization of an acute in vivo mouse model for effects of mutant FUS expression in astrocytes. (a) Model design: Left: Image of mouse cervical spinal region indicating the AAV delivery site. Dotted black line indicates distance from midline that injections occur to appropriately target ventral horns. White arrows indicate injection locations for two spinal levels. Right: Cartoon of spinal cord region within the context of the total cord. Six injections are delivered bi-laterally from C4 to C6 region. (b) Representative transduction profile showing 10× magnification images (scale bar indicates 500 μm) and cropped 20× magnification images (scale bar indicates 150 μm) of eGFP (left) and eGFP:hFUS<sup>R521G</sup> (right; mtFUS) in 30 μm spinal cord slices within the transduction region after six  $1 \times 10^{11}$  GC injections in p180 female wildtype mice. Images at 10× and 20× are from independent animals, demonstrating comparable and reproducible results. Internal dotted lines mark dorsal and ventral horns, external dotted lines mark the outer border of the spinal cord. (c) Transduction efficiency comparisons of eGFP and mtFUS viruses after 7 days of transduction. Quantification of GFP<sup>+</sup> cells within the ventral spinal cord compared between eGFP and mtFUS expressing animals. Assessment revealed comparable numbers of cells transduced with virus under both viral vectors using the paradigm and viral dosing parameters indicated in B. For these evaluations  $n = 3$  mice per condition (eGFP or mtFUS) were assessed, with 5–10 spinal cord sections analyzed per each subject. Data presented as mean  $\pm$  SEM. (d) Representative immunohistochemical staining of cell-type specific markers in 30 μm spinal cord sections of mice 7 days post-injection, 60× magnification, scale bar indicates 50 μm. The cell types tested are astrocytes (GFAP), neurons (NeuN), microglia (Iba1) and oligodendrocytes (Olig2). Cell type specific markers are shown in red, with GFP<sup>+</sup> cells indicating those which were transduced with virus. White arrows indicate co-positive cells. (e) Quantification of the percentage GFP<sup>+</sup> labeled with each cell lineage marker. GFP<sup>+</sup> cells are represented by 92.11% astrocytes, 6.45% neurons, 1.08% oligodendrocytes, and 0.36% microglia

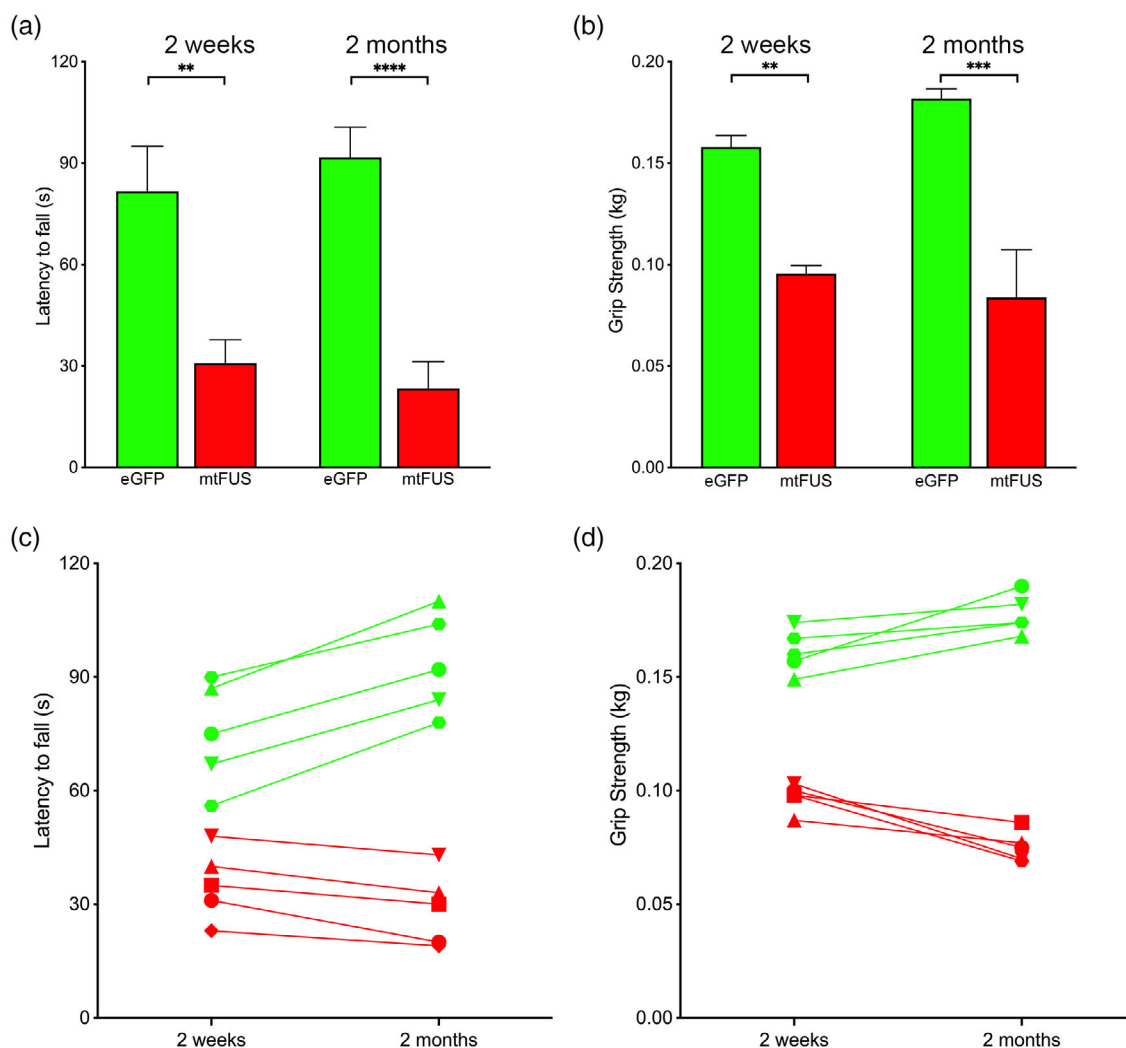


**FIGURE 2** Motor deficits occur when mtFUS is expressed in astrocytes. (a) Quantification of motor behavior by wire hang latency, in eGFP and mtFUS mice at 2-weeks and 2-months months post-injection. At 2-weeks, animals expressing mtFUS had a significantly reduced wire hang latency, compared with eGFP animals. This was a permanent effect, as at 2-months, mtFUS animals again showed a significantly reduced latency compared with eGFP animals. Data presented as mean  $\pm$  SEM,  $n = 5$  animals per timepoint per condition. Dunnett's multiple comparison test determined statistical significance for comparison of GFP versus mtFUS at each timepoint,  $**p < .01$ ,  $****p < .0001$ . (b) Forelimb grip-strength was also assessed in eGFP and mtFUS animals at 2 weeks post-injection and 2-months post injection. At 2-weeks, mtFUS expressing animals had a significantly reduced grip strength compared with eGFP animals. This also was a permanent effect, at 2-months, mtFUS animals again showed a significantly reduced grip strength compared with eGFP animals. Data presented as mean  $\pm$  SEM,  $n = 5$  animals per timepoint per condition. Dunnett's multiple comparison test determined statistical significance for comparison of GFP versus mtFUS at each timepoint,  $**p < .01$ ,  $***p < .001$ . (c) Wire hang latency was compared in individual animals across the 2-week and 2-point timepoints post-injection. While eGFP expressing animals each displayed progressive increases in wire hang latency to fall endurance, mtFUS expressing animals had a reduction in performance between the two timepoints. Data presented as mean at each timepoint,  $n = 5$  animals per condition. Green shapes represent individual eGFP expressing animals, while red shapes represent individual mtFUS expressing animals. (d) Forelimb grip-strength was also compared in individual animals across the 2-week and 2-point timepoints post-injection. Similar to wire hang latency results, while eGFP expressing animals each displayed progressive increases in grip strength over time, mtFUS expressing animals had a reduction in strength measurements between the two timepoints. Data presented as mean at each timepoint,  $n = 5$  animals per condition. Green shapes represent individual eGFP expressing animals, while red shapes represent individual mtFUS expressing animals

choline acetyltransferase (ChAT) which marks all cholinergic motor neurons. At the 3-day post-injection timepoint prior to overt symptoms, we do not observe a loss of MMP9<sup>+</sup> cells (Figure S3a). However, at the 2-week timepoint when we do observe motor symptoms, there is a loss of MMP9<sup>+</sup> cells in mtFUS mice, corresponding to only 59.6%  $\pm$  8.5% of that found in sham surgery ( $p < .01$ ) and eGFP

animals ( $p < .05$ ) (Figure 3a,c). Further, we see a similar temporal pattern of ChAT<sup>+</sup> cell loss in mtFUS expressing animals, with similar ChAT levels among groups at 3 days post-injection, which is reduced significantly in mtFUS mice at the 2-week time point, falling to 51.5%  $\pm$  3.0% of sham surgery ( $p < .05$ ) and eGFP animals ( $p < .05$ ) (Figures 3b,d and S3b). We also evaluated whether progression of

motor neuron loss occurred between our 2 week and 2 month end-point groups. When MMP9<sup>+</sup> cells were assessed, sham surgery and eGFP groups did not have reduction in motor neuron counts, with

1.2% ± 1.8% and 1.1% ± 1.9% reductions respectively. mtFUS animals however had a large loss of motor neurons between the two timepoints, further reducing motor neuron counts by 30.3% ± 1.4%

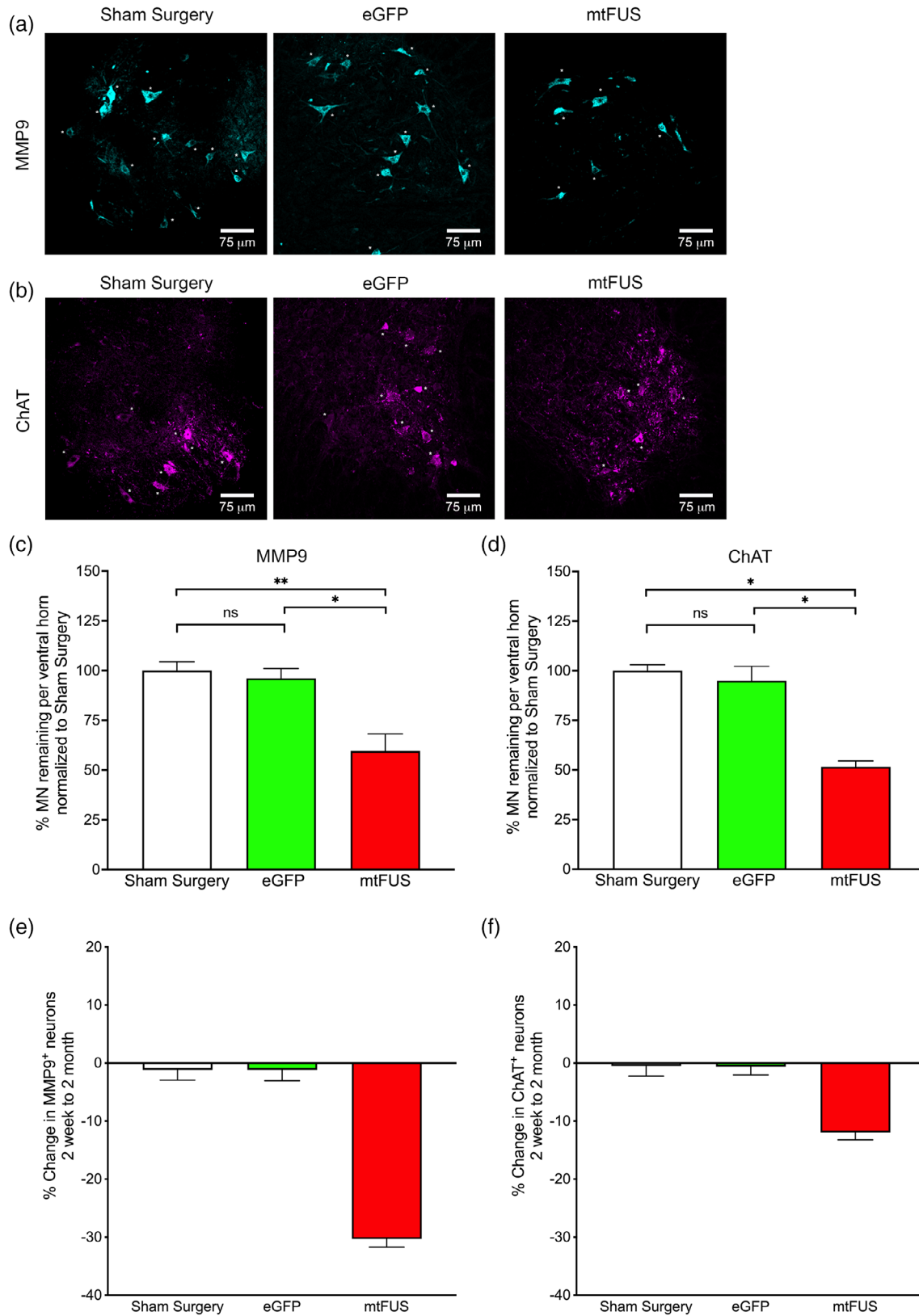
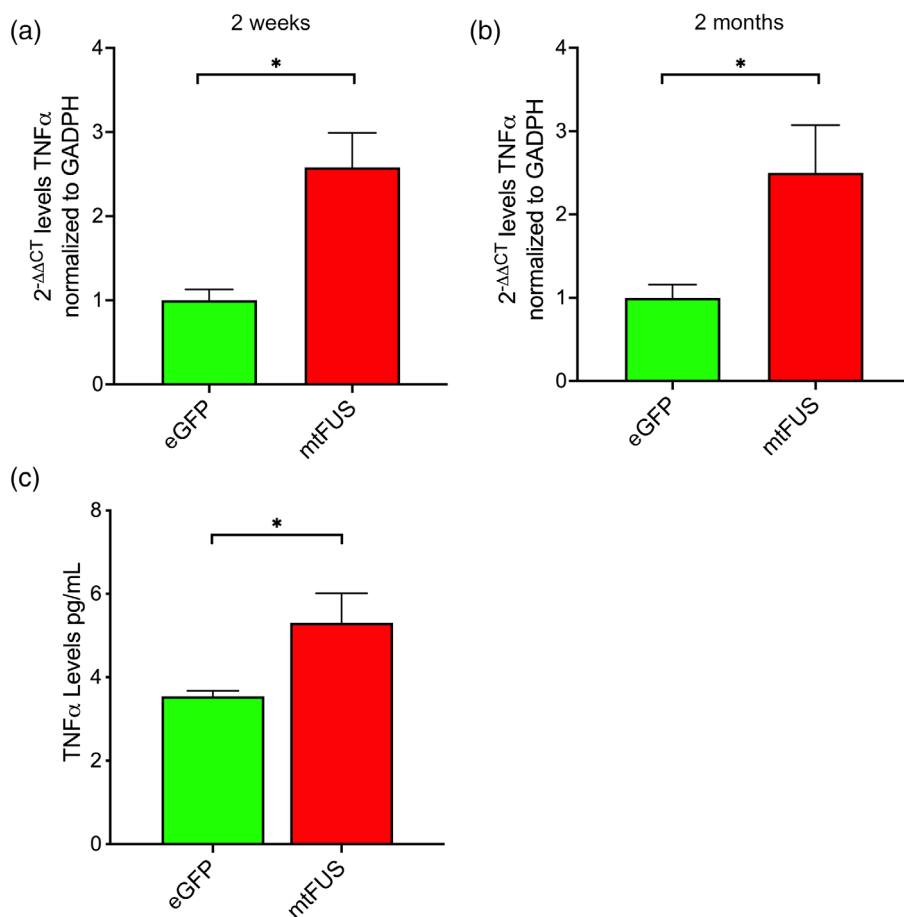


FIGURE 3 Legend on next page.



**FIGURE 4** TNF $\alpha$  levels are elevated in mtFUS mice. (a) qPCR analysis of TNF $\alpha$  levels at 2 weeks post-injection indicates a significantly elevated level of expression in mtFUS expressing animals compared with eGFP controls. Data shown as relative fold-changes compared to eGFP alone, and are presented as mean  $\pm$  SEM, Student's *t* test determined statistical significance,  $n = 5$  animals per group,  $*p < .05$ . (b) qPCR analysis of TNF $\alpha$  levels at 2 months post-injection indicates a significantly elevated level of expression in mtFUS expressing animals compared with eGFP controls. Data shown as relative fold-changes compared to eGFP alone, and are presented as mean  $\pm$  SEM, Student's *t* test determined statistical significance,  $n = 5$  animals per group,  $*p < .05$ . (c) A highly sensitive quantitative TNF $\alpha$  ELISA was performed to assess soluble TNF $\alpha$  levels in animals expressing eGFP or mtFUS for 2-weeks. A significant increase in TNF $\alpha$  was detected in mtFUS animals. Data presented as mean  $\pm$  SEM, Student's *t*-test determined statistical significance,  $n = 6$  animals per group,  $*p < .05$

(Figure 3e). Analysis of ChAT<sup>+</sup> cells revealed a similar outcome, with sham surgery and eGFP animals having minimal 0.49%  $\pm$  1.8% and 0.61%  $\pm$  1.4% ChAT<sup>+</sup> cell loss respectively, while the mtFUS animals had a progressive reduction losing an additional 12.0%  $\pm$  1.3% of

ChAT<sup>+</sup> cells (Figure 3f). These results provide evidence that astrocyte-restricted mtFUS expression in adult mice can cause motor neuron dysfunction and death in as little as 2 weeks, and that progressive motor degeneration continues to occur with time.

**FIGURE 3** Progressive loss of motor neurons takes place when mtFUS is expressed in astrocytes. (a) Immunohistochemical staining for MMP9, a marker for vulnerable large motor-neurons in ALS, in spinal cord sections at 14 days post-injection. Sham surgery and eGFP expressing animals show similar numbers of MMP9<sup>+</sup> neurons visualized in cyan, while in mtFUS animals there are fewer positive cells. Representative fields from 60 $\times$  magnification z-stack confocal images, scale bar indicates 75  $\mu$ m. (b) Immunohistochemical staining for the motor neuron marker ChAT at 14 days post-injection. Sham surgery and eGFP expressing animals show similar numbers of ChAT<sup>+</sup> neurons visualized in magenta and indicated by \*, while in mtFUS animals there are fewer positive cells. Representative fields from 60 $\times$  magnification z-stack confocal images, scale bar indicates 75  $\mu$ m. (c) MMP9<sup>+</sup> motor neurons were quantified within the ventral horn of spinal cord sections by manual counting of immunopositive cells within the ventral horn region. Analysis revealed a significant reduction in MMP9<sup>+</sup> cells in mtFUS expressing animals compared with either sham surgery controls ( $**p < .01$ ) or eGFP expressing animals ( $*p < .05$ ). Data presented as mean  $\pm$  SEM,  $n = 5$  animals per condition,  $m = 4$  ventral horns per animal. Sidak's multiple comparison test determined statistical significance. (d) ChAT<sup>+</sup> motor neurons were also quantified within the ventral horn of spinal cord sections by manual counting of immunopositive cells within the ventral horn region. Quantification showed a significant reduction in ChAT<sup>+</sup> cells in mtFUS expressing animals compared with either sham surgery controls ( $*p < .05$ ) or eGFP expressing animals ( $*p < .05$ ). Data presented as mean  $\pm$  SEM,  $n = 5$  animals per condition,  $m = 4$  ventral horns per animal. Sidak's multiple comparison test determined statistical significance. (e) The number of MMP9<sup>+</sup> motor neurons was compared in each experimental group between the 2-week and 2-month timepoints. Sham surgery and eGFP expressing animals did not have any appreciable change in the number of MMP9<sup>+</sup> cells between these time points. In contrast, MMP9<sup>+</sup> motor neurons were reduced by 30.3% in mtFUS expressing animals. Data presented as mean  $\pm$  SEM,  $n = 5$  animals per condition,  $m = 4$  ventral horns per animal. (f) The number of ChAT<sup>+</sup> motor neurons was also compared in each experimental group between the 2-week and 2-month timepoints. While sham surgery and eGFP expressing animals did not have any appreciable change in the number of ChAT<sup>+</sup> cells between these time points, ChAT<sup>+</sup> motor neurons were reduced by 12.0% in mtFUS expressing animals. Data presented as mean  $\pm$  SEM,  $n = 5$  animals per condition,  $m = 4$  ventral horns per animal

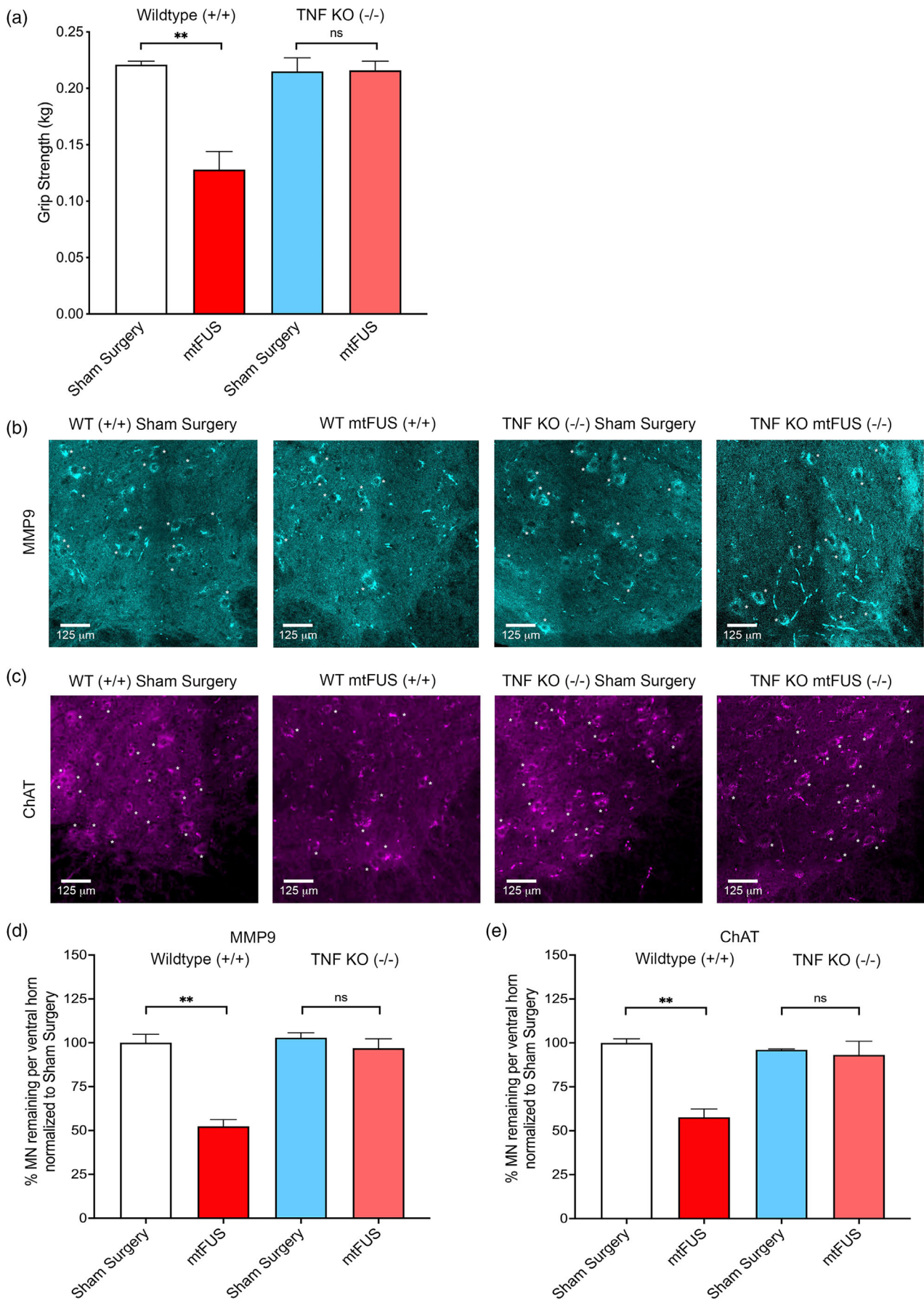


FIGURE 5 Legend on next page.



### 3.3 | TNF $\alpha$ levels are elevated in mtFUS mice

Next, we sought to determine whether TNF $\alpha$  signaling was altered in mtFUS animals as we had previously observed *in vitro* (Kia et al., 2018). Using qRT-PCR analysis on cervical spinal cord sections of animals 2 weeks post-injection, we found significantly elevated TNF $\alpha$  mRNA expression in mtFUS mice, with levels  $2.6 \pm 0.41$ -fold higher than animals expressing eGFP ( $p < .05$ ) (Figure 4a). Similarly, qRT-PCR was performed on spinal cord sections of animals 2 months post-injection. In these animals, TNF $\alpha$  mRNA expression was still elevated in mtFUS mice, with levels  $2.5 \pm 0.57$ -fold higher than animals expressing eGFP ( $p < .05$ ) (Figure 4b). Additionally, the soluble fraction from cervical spinal cord homogenates was analyzed with a highly sensitive TNF $\alpha$  ELISA, which revealed a significantly increased level of secreted TNF $\alpha$  protein in mtFUS animals compared with eGFP control animals 2 weeks post-injection, with  $3.5 \pm 0.14$  pg/ml detected in eGFP animals, and  $5.3 \pm 0.7$  pg/ml detected in mtFUS animals ( $p < .05$ ) (Figure 4c).

This elevation of TNF $\alpha$  corresponded with increased astrocyte reactivity as measured by glial fibrillary acidic protein (GFAP) at the mRNA level, where a  $3.0 \pm 0.46$ -fold increase was seen ( $p < .001$ ) (Figure S4a), and at the protein level through enhanced signal via immunofluorescent staining when compared with eGFP control animals (Figure S4b). Enhanced astrocyte reactivity was also indicated by an elevation of GFAP $^+$  cells per ventral horn, with mtFUS animals having 1.68-fold more astrocytes per ventral horn compared to eGFP and sham surgery groups ( $p < .001$ ) (Figure S4c). These data suggest that astrocytic mtFUS expression leads to pro-inflammatory changes *in vivo*, which include elevated TNF $\alpha$  levels and subsequent astrocytic reactivity in the surrounding region.

### 3.4 | TNF $\alpha$ knockout animals do not display motor deficits or loss of motor neurons when mtFUS is expressed in astrocytes

We next sought to explore whether the behavioral and motor neuron phenotypes that we observed were explicitly caused by the action of secreted TNF $\alpha$  *in vivo*. To study this, we repeated intraspinal delivery of eGFP or mtFUS in p180 homozygous TNF $\alpha$  knockout (TNF KO) and paired wildtype (TNF $^{+/+}$ ) animals. At 2 weeks post-injection, these animals were evaluated for grip strength and assessed for spinal cord motor neuron number by MMP9 and ChAT staining as done in Figure 2. In striking contrast to the paired wildtype (TNF $^{+/+}$ ) controls expressing mtFUS, which displayed a significant reduction from 0.22 to 0.13 kg grip strength ( $p < .01$ ), TNF $\alpha$  knockout animals receiving mtFUS did not have any deficits in grip strength, with comparable measurements of 0.22 kg in both sham surgery and mtFUS expressing groups (Figure 5a). Moreover, while wildtype TNF $^{+/+}$ -mtFUS animals again showed reductions in MMP9 $^+$  and ChAT $^+$  cells (to 52.4% and 57.7% in mtFUS versus sham surgery wildtype animals respectively ( $p < .01$ )), we also did not observe any decrease in MMP9 $^+$  or ChAT $^+$  motor neurons in the spinal cord of TNF $\alpha$  knockout animals, with values of 96.9% MMP9 $^+$  and 97.0% ChAT $^+$  cells respectively in mtFUS compared with sham surgery animals (Figure 5b-e). Reactive astrogliosis was also assessed in this cohort through staining and quantification of GFAP $^+$  cells per ventral horn of TNF $^{+/+}$  or TNF $\alpha$  knockout animals undergoing sham surgery or expressing mtFUS (Figure 6). In contrast to the significantly elevated 1.58-fold change of GFAP $^+$  astrocytes in mtFUS expressing TNF $\alpha^{+/+}$  animals ( $p < .001$ ), TNF $\alpha$  knockout animals did not have elevation of GFAP $^+$  cell number following mtFUS expression, with the number of reactive astrocytes being

**FIGURE 5** TNF $\alpha$  knockout animals do not display motor deficits or loss of motor neurons when mtFUS is expressed in astrocytes. (a) Forelimb grip-strength was quantified in an age-matched paired cohort of wildtype and TNF $\alpha$  knockout (TNF KO) mice at 2-weeks following either sham surgery or mtFUS expression. At this time, mtFUS expressing animals in the wildtype (TNF $^{+/+}$ ) cohort had a significantly reduced grip strength of 0.13 kg, compared with sham surgery animals with a grip strength of 0.22 kg. In contrast, in the TNF KO cohort, animals displayed comparable grip strength values of 0.22 kg regardless of whether they had undergone sham surgery or were expressing mtFUS. Data presented as mean  $\pm$  SEM,  $n = 3$  animals per timepoint per condition. Dunnett's multiple comparison test determined statistical significance for comparison of sham versus mtFUS for each genotype,  $**p < .01$ . (b) Representative immunohistochemical staining for MMP9 (cyan) in spinal cord sections from wildtype and TNF KO animals having undergone sham surgery or expressing mtFUS at 14 days post-injection. In wildtype animals, mtFUS expressing animals show a reduction in numbers of MMP9 $^+$  neurons. In TNF KO animals, comparable numbers of MMP9 $^+$  cells are seen both in the sham surgery and mtFUS conditions (indicated by \*). Representative fields from 60 $\times$  magnification z-stack confocal images, scale bar indicates 125  $\mu$ m. (c) Representative immunohistochemical staining for ChAT (magenta) at 14 days post-injection from wildtype and TNF KO animals having undergone sham surgery or expressing mtFUS. In wildtype animals, mtFUS expressing animals show a reduction in numbers of ChAT $^+$  neurons. In TNF KO animals, comparable numbers of ChAT $^+$  cells are seen both in the sham surgery and mtFUS conditions (indicated by \*). Representative fields from 60 $\times$  magnification z-stack confocal images, scale bar indicates 125  $\mu$ m. (d) Quantification of MMP9 $^+$  motor neurons was performed as in Figure 2. Analysis revealed a significant reduction in MMP9 $^+$  cells in wildtype animals expressing mtFUS compared to wildtype sham surgery animals ( $**p < .01$ ). In contrast, comparable numbers of MMP9 $^+$  cells were found in both sham surgery and mtFUS animals in the TNF KO cohort. Data presented as mean  $\pm$  SEM,  $n = 5$  animals per condition,  $m = 4$  ventral horns per animal. Sidak's multiple comparison test determined statistical significance. (e) Quantification of ChAT $^+$  motor neurons was performed as in Figure 2. A significant decrease in ChAT $^+$  motor neurons was observed in wildtype animals expressing mtFUS compared to their paired sham surgical controls ( $**p < .01$ ). However, similar numbers of ChAT $^+$  cells were found in both the sham surgery and mtFUS groups for the TNF KO cohort. Data presented as mean  $\pm$  SEM,  $n = 5$  animals per condition,  $m = 4$  ventral horns per animal. Sidak's multiple comparison test determined statistical significance

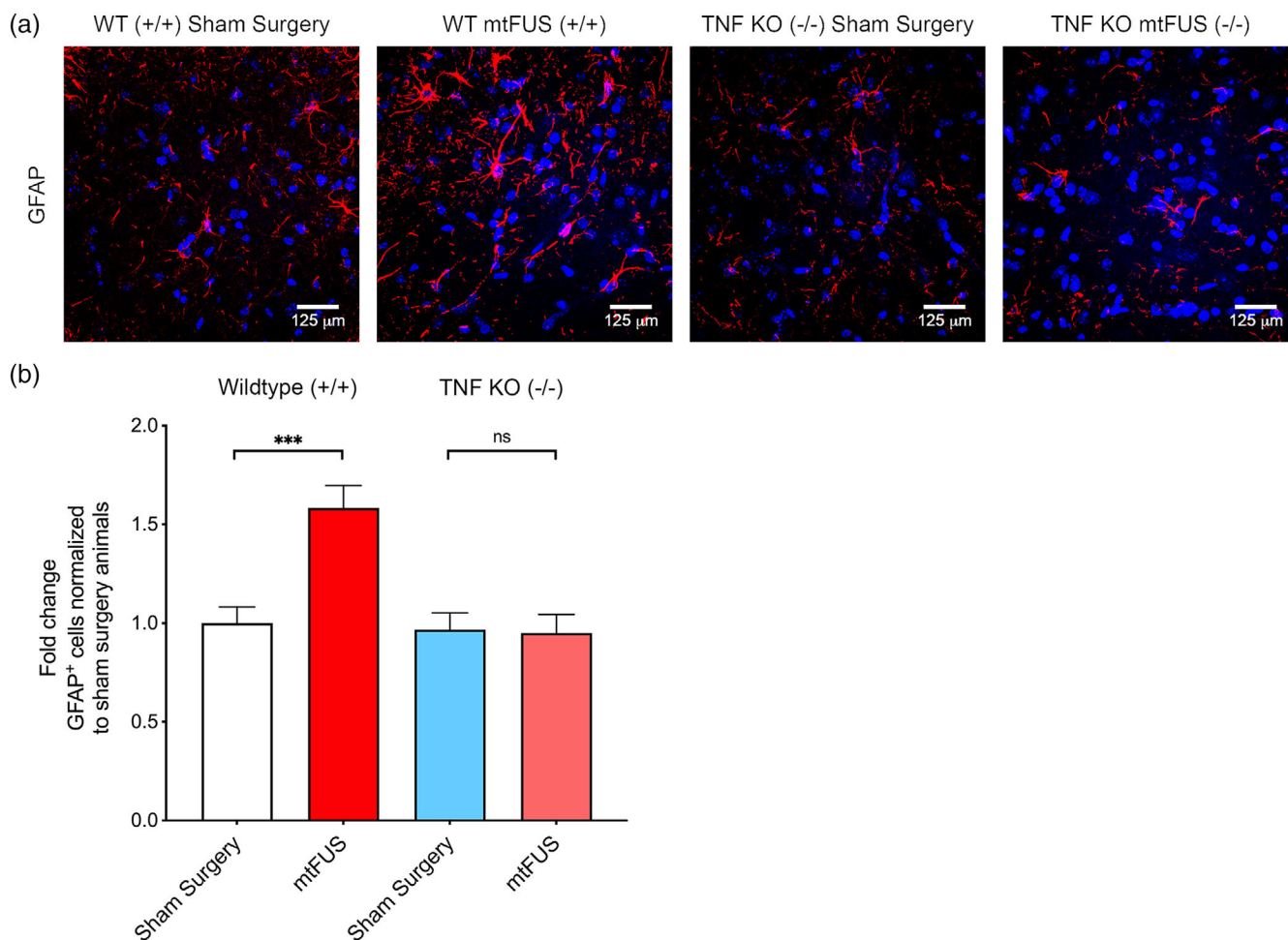


**FIGURE 6** TNF $\alpha$  knockout animals do not have elevated numbers of reactive astrocytes. (a) Representative immunohistochemical staining for GFAP (red) in spinal cord sections from wildtype and TNF KO animals having undergone sham surgery or expressing mtFUS at 14 days post-injection. In wildtype animals, mtFUS expressing animals show an increase in GFAP<sup>+</sup> astrocytes. In TNF KO animals, comparable numbers of GFAP<sup>+</sup> cells are seen both in the sham surgery and mtFUS conditions. Representative fields from 60 $\times$  magnification z-stack confocal images, scale bar indicates 125  $\mu$ m. (b) Quantification of GFAP<sup>+</sup> astrocytes was performed by counting number of immunopositive cells per ventral horn, expressed as fold change normalized to wildtype animal sham surgery controls. Analysis revealed a significant elevation in GFAP<sup>+</sup> astrocytes in wildtype animals expressing mtFUS compared to wildtype sham surgery animals (\*\* $p < .001$ ). In contrast, comparable numbers of GFAP<sup>+</sup> cells were found in both sham surgery and mtFUS animals in the TNF KO cohort. Data presented as mean  $\pm$  SEM,  $n = 5$  animals per condition,  $m = 4$  ventral horns per animal. Sidak's multiple comparison test determined statistical significance

maintained at comparable levels to TNF<sup>+/+</sup> sham surgery levels in either experimental group (Figure 6b). This data, along with the results presented in Figure S4, taken together prove that the elevation of TNF $\alpha$  in our model is the direct result of mtFUS expression in those cells, rather than a secondary effect caused by reactive astrogliosis resulting from surgery or general exogenous protein expression. Genotype was confirmed in these animals by PCR analysis to verify TNF $\alpha$  knockout (Figure S5a). Comparable levels of mtFUS expression was also validated in wildtype TNF<sup>+/+</sup> and TNF $\alpha$  knockout animals receiving mtFUS virus by qRT-PCR analysis ( $p < .001$ ) (Figure S5b). Overall, these findings suggest that TNF $\alpha$  signaling is substantially responsible for the observed motor behavioral deficits and motor neuron cell death that is caused in our mouse model.

### 3.5 | $\alpha$ -TNF $\alpha$ neutralizing antibody application at the time of mtFUS injection prevents motor neuron death and functional deficits in mtFUS expressing animals

Next, we tested whether pharmacological manipulation of TNF $\alpha$  could also prevent motor dysfunction and motor neuron death in our mouse model. For this study, we have applied a TNF $\alpha$  neutralizing antibody at an effective dosing of 2 mg/kg, as has been reported in other in vivo experimental models (Finsterbusch et al., 2016; Via et al., 2001). First, we evaluated the consequences of co-administering the TNF $\alpha$  neutralizing antibody at the time of viral injection. In this paradigm, antibody was co-injected with AAV, while maintaining the same 1  $\mu$ l total injection volume and viral titer as in previous cohorts. At

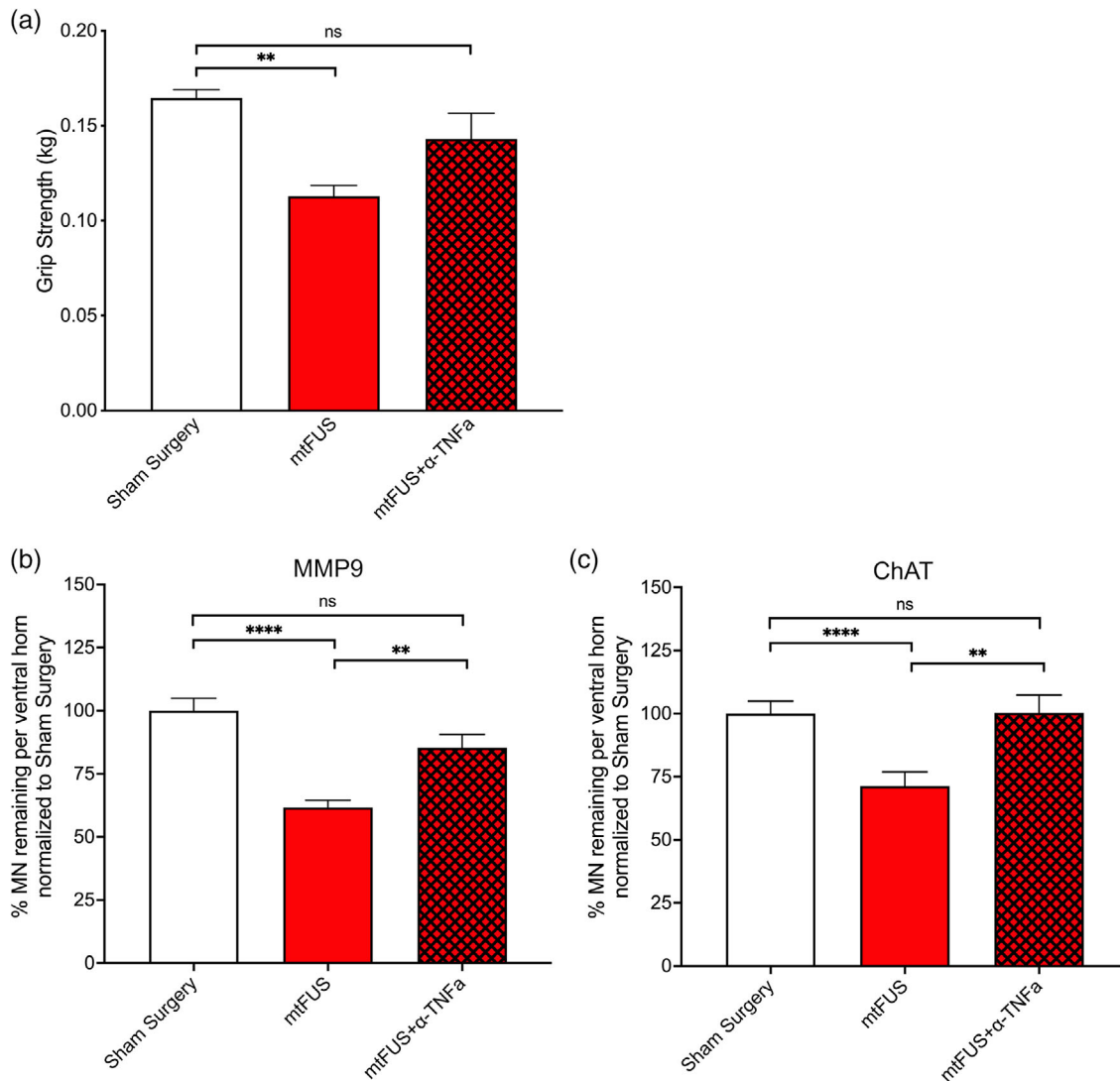


**FIGURE 7**  $\alpha$ -TNF $\alpha$  neutralizing antibody application at the time of mtFUS injection prevents motor neuron death and functional deficits in mtFUS expressing animals. (a) Forelimb grip-strength was quantified in a cohort containing sham surgery animals, mtFUS expressing animals, and mtFUS expressing animals that received  $\alpha$ TNF $\alpha$  neutralizing antibody (mtFUS+  $\alpha$ -TNF $\alpha$ ) at the time of viral delivery, 2 weeks after intraspinal injections. mtFUS expressing animals had a significantly reduced grip strength compared with sham surgery animals, as had been previously seen. In the mtFUS+  $\alpha$ -TNF $\alpha$  cohort however, animals displayed grip strength values which did not statistically differ compared with the sham surgery group. Data presented as mean  $\pm$  SEM,  $n = 6$  animals per timepoint per condition. One-way ANOVA with Sidak's multiple comparison test determined statistical significance (\*\* $p < .01$ ). (b) Quantification of MMP9<sup>+</sup> motor neurons was performed as in Figure 2. As previously noted, analysis revealed a significant reduction in MMP9<sup>+</sup> cells in wildtype animals expressing mtFUS compared to wildtype sham surgery animals (\*\*\*\* $p < .0001$ ). In contrast, mtFUS expressing animals which received  $\alpha$ -TNF $\alpha$  neutralizing antibody showed a significant restoration of MMP9<sup>+</sup> compared with the mtFUS only group (\*\* $p < .01$ ) and had levels that were not statistically altered from the sham surgery cohort. Data presented as mean  $\pm$  SEM,  $n = 6$  animals per condition,  $m = 4$  ventral horns per animal. One-way ANOVA with Sidak's multiple comparison test determined statistical significance. (c) Quantification of ChAT<sup>+</sup> motor neurons was performed as in Figure 2. A significant decrease in ChAT<sup>+</sup> motor neurons was again seen in animals expressing mtFUS compared to the sham surgical controls (\*\* $p < .01$ ). mtFUS+  $\alpha$ -TNF $\alpha$  animals showed a significant restoration of ChAT<sup>+</sup> compared with the mtFUS only group (\*\* $p < .01$ ) and had levels that were not statistically altered from the sham surgery cohort. Data presented as mean  $\pm$  SEM,  $n = 6$  animals per condition,  $m = 4$  ventral horns per animal. One-way ANOVA with Sidak's multiple comparison test determined statistical significance

2 weeks post-injection, animals receiving mtFUS virus + TNF $\alpha$  neutralizing antibody ( $\alpha$ -TNF $\alpha$ ) displayed similar grip strength to their control sham surgery counterparts (0.14 kg compared to 0.16 kg), while mtFUS only animals demonstrated the same significant grip strength deficit as observed in earlier cohorts (0.11 kg) ( $p < .01$ ) (Figure 7a).

Additionally, animals which received mtFUS+  $\alpha$ -TNF $\alpha$  had preserved motor neuron numbers comparable to sham surgical controls (MMP9<sup>+</sup> 85.3% and ChAT 100.2% respectively), while animals which received mtFUS alone showed significant reductions as previously observed (MMP9<sup>+</sup> 61.7%, sham vs mtFUS  $p < .0001$ , mtFUS+

$\alpha$ -TNF $\alpha$  vs mtFUS  $p < .01$ ; ChAT<sup>+</sup> 71.3%, sham vs mtFUS  $p < .01$ , mtFUS+  $\alpha$ -TNF $\alpha$  vs mtFUS  $p < .01$ ) (Figure 7b,c). In this surgical paradigm, we have confirmed that  $\alpha$ -TNF $\alpha$  had no effect on levels of

mtFUS expression by qRT-PCR analysis ( $p < .01$ ) (Figure S6a). From this cohort of animals, we have observed that when  $\alpha$ -TNF $\alpha$  is administered concomitant with intraspinal mtFUS virus delivery, effects on

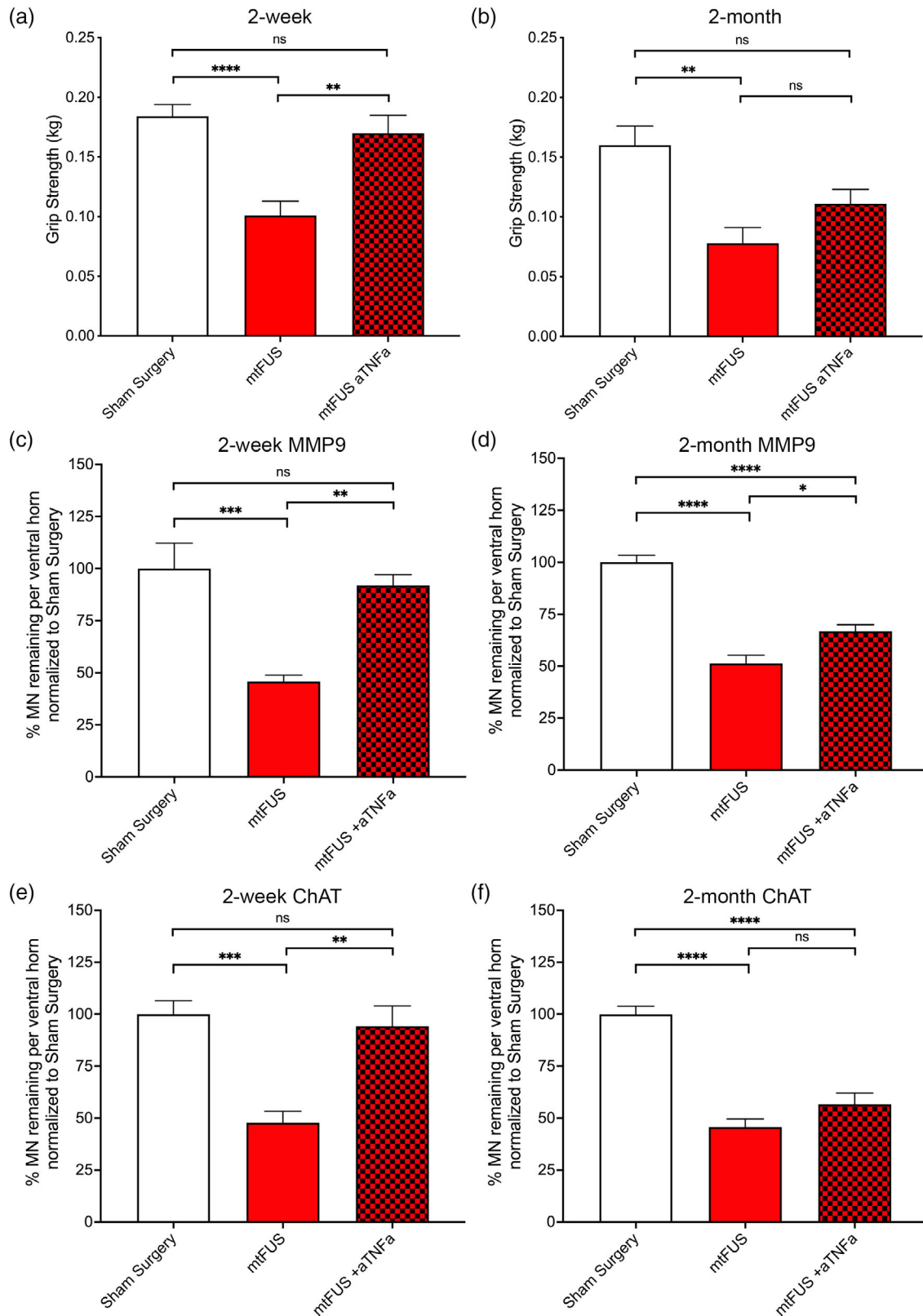


FIGURE 8 Legend on next page.

motor neuron dysfunction and death are greatly attenuated, such that animals display no overt motor deficits or loss of motor neurons.

### 3.6 | $\alpha$ -TNF $\alpha$ neutralizing antibody application 1 week following mtFUS injection prevents motor neuron death and functional deficits in mtFUS expressing animals for a period of time

Finally, we assessed the effects of administering TNF $\alpha$  neutralizing antibody after a period of mtFUS expression, to better understand if this could be a viable therapeutic approach when mtFUS is already present and evoking cellular effects. In designing this paradigm, we chose to investigate outcomes of a single application of neutralizing antibody to quickly ascertain whether blocking TNF $\alpha$ -mediated effects would have any utility if mtFUS was already perturbing the system. In this surgical paradigm, mtFUS intraspinal injections were performed as in all previous cohorts, with a non-adhesive dressing applied over the site of spinal cord injections just prior to surgical closure. Following 1 week of recovery and mtFUS expression, animals underwent a second surgery in which the spinal cord was again exposed at the same location, the dressing was removed, and was replaced with an absorbable gelatin sponge soaked in sterile saline +/-

$\alpha$ -TNF $\alpha$ . Animals were allowed to recover and were assessed for grip strength and motor neuron numbers at a 2-week endpoint following this second surgery. At 2 weeks following  $\alpha$ -TNF $\alpha$  administration we observed grip strength, MMP9<sup>+</sup>, and ChAT<sup>+</sup> neurons which were comparable to sham surgery animals and which were significantly restored compared to mtFUS animals which had not received neutralizing antibody (Figure 8). At this timepoint, mtFUS only expressing animals displayed a significant reduction of grip strength from 0.18 kg to 0.10 kg ( $p < .0001$ ), however, animals receiving  $\alpha$ -TNF $\alpha$  following 1 week of mtFUS expression had a significantly elevated measured grip strength of 0.17 kg ( $p < .01$ ) (Figure 8a). Similarly, while MMP9<sup>+</sup> cells fell to 45.8% in mtFUS only animals at 2 weeks ( $p < .001$ ), those also receiving  $\alpha$ -TNF $\alpha$  still had 91.9% of cells compared with sham surgery animals, a significant increase over the mtFUS animals ( $p < .01$ ) (Figure 8c). Likewise, when ChAT<sup>+</sup> cells were evaluated, mtFUS only animals had a significant reduction in cell number (47.8%) ( $p < .001$ ), mtFUS +  $\alpha$ -TNF $\alpha$  animals showed a significant recovery of cell number, comparable to that of sham surgery animals (94.2%,  $p < .01$ ) (Figure 8e). Given this striking result following 2-weeks of  $\alpha$ -TNF $\alpha$  application, we extended our trials in an additional cohort to determine if animals retained motor neuron functionality and viability 2-months after delivery of the single-dose application of  $\alpha$ -TNF $\alpha$  neutralizing antibody. In contrast to our 2-week results, at 2 months grip

**FIGURE 8**  $\alpha$ -TNF $\alpha$  neutralizing antibody application 1 week following mtFUS injection prevents motor neuron death and functional deficits for a period of time. (a) In the paradigm of viral infection with mtFUS, followed a week later by  $\alpha$ -TNF $\alpha$  neutralizing antibody application, forelimb grip-strength was quantified 2 weeks after administration of  $\alpha$ -TNF $\alpha$ . mtFUS expressing animals had a significantly reduced grip strength compared with sham surgery animals (\*\*\*\* $p < .0001$ ). In the mtFUS+  $\alpha$ -TNF $\alpha$  cohort, animals displayed grip strength which significantly elevated compared with the mtFUS only animals (\*\* $p < .01$ ), and which did not statistically differ compared with the sham surgery group. Data presented as mean  $\pm$  SEM,  $n = 6$  animals per timepoint per condition. One-way ANOVA with Sidak's multiple comparison test determined statistical significance. (b) In this same paradigm, forelimb grip-strength was quantified 2 months after application of  $\alpha$ -TNF $\alpha$ . mtFUS expressing animals had a significantly reduced grip strength of 0.08 kg compared with sham surgery animals with a grip strength of 0.16 kg (\*\* $p < .01$ ). By this time, the mtFUS+  $\alpha$ -TNF $\alpha$  cohort also displayed grip strength reduction, with values of 0.11 kg, which trended towards a significant reduction compared with sham surgery controls ( $p = .13$ ), and which was not statistically different compared with the mtFUS only animals. Data presented as mean  $\pm$  SEM,  $n = 6$  animals per timepoint per condition. One-way ANOVA with Sidak's multiple comparison test determined statistical significance. (c) Quantification of MMP9<sup>+</sup> motor neurons was performed as in Figure 2 for our delayed  $\alpha$ -TNF $\alpha$  surgical group. At 2 weeks following neutralizing antibody application, analysis revealed a significant reduction in MMP9<sup>+</sup> cells in animals expressing mtFUS only compared to sham surgery animals (\*\* $p < .001$ ). In contrast, mtFUS expressing animals which received  $\alpha$ -TNF $\alpha$  neutralizing antibody showed a significant restoration of MMP9<sup>+</sup> compared with the mtFUS only group (\*\* $p < .01$ ) and had levels that were not statistically altered from the sham surgery cohort. Data presented as mean  $\pm$  SEM,  $n = 6$  animals per condition,  $m = 4$  ventral horns per animal. One-way ANOVA with Sidak's multiple comparison test determined statistical significance. (d) Quantification of MMP9<sup>+</sup> motor neurons was performed as in Figure 2 for our delayed  $\alpha$ -TNF $\alpha$  surgical group at 2 months following  $\alpha$ -TNF $\alpha$  antibody application. Analysis showed a significant reduction in MMP9<sup>+</sup> cells in animals expressing mtFUS only compared to sham surgery animals (\*\*\*\* $p < .0001$ ). By this time, mtFUS expressing animals which received  $\alpha$ -TNF $\alpha$  neutralizing antibody also showed a significant reduction in MMP9<sup>+</sup> cells compared with the sham surgery group (\*\*\*\* $p < .0001$ ) and had levels that were only slightly elevated compared with the mtFUS only group (\* $p < .05$ ). Data presented as mean  $\pm$  SEM,  $n = 6$  animals per condition,  $m = 4$  ventral horns per animal. One-way ANOVA with Sidak's multiple comparison test determined statistical significance. (e) Quantification of ChAT<sup>+</sup> motor neurons was performed as in Figure 2 for our delayed  $\alpha$ -TNF $\alpha$  surgical group. At 2 weeks following neutralizing antibody application, analysis revealed a significant reduction in ChAT<sup>+</sup> cells in animals expressing mtFUS only compared to sham surgery animals (\*\*\*\* $p < .001$ ). In contrast, mtFUS expressing animals which received  $\alpha$ -TNF $\alpha$  neutralizing antibody showed a significant restoration of ChAT<sup>+</sup> compared with the mtFUS only group (\*\* $p < .01$ ) and had levels that were not statistically altered from the sham surgery cohort. Data presented as mean  $\pm$  SEM,  $n = 6$  animals per condition,  $m = 4$  ventral horns per animal. One-way ANOVA with Sidak's multiple comparison test determined statistical significance. (f) Quantification of ChAT<sup>+</sup> motor neurons was performed as in Figure 2 for our delayed  $\alpha$ -TNF $\alpha$  surgical group at 2 months following  $\alpha$ -TNF $\alpha$  antibody application. Analysis showed a significant reduction in ChAT<sup>+</sup> cells in animals expressing mtFUS only compared to sham surgery animals (\*\*\*\* $p < .0001$ ). By this time, mtFUS expressing animals which received  $\alpha$ -TNF $\alpha$  neutralizing antibody also showed a significant reduction in ChAT<sup>+</sup> cells compared with the sham surgery group (\*\*\*\* $p < .0001$ ) and had levels that were comparable to the mtFUS only group. Data presented as mean  $\pm$  SEM,  $n = 6$  animals per condition,  $m = 4$  ventral horns per animal. One-way ANOVA with Sidak's multiple comparison test determined statistical significance

strength was reduced from 0.16 to 0.11 kg and no longer had a significant recovery from the mtFUS animals (0.08 kg) (Figure 8b). Additionally, both MMP9<sup>+</sup> (66.8%) and ChAT<sup>+</sup> cells (56.7%) were significantly reduced compared to sham surgery ( $p < .0001$ ), and instead were comparable to mtFUS animals that had not received neutralizing antibody (Figure 8d,f). In this surgical paradigm, levels of mtFUS expression were again confirmed to be comparable in mtFUS and mtFUS+ $\alpha$ -TNF $\alpha$  groups by qRT-PCR analysis at both 2-week and 2-month evaluation timepoints (Figure S6b). In conclusion, we have found that a single dosing of  $\alpha$ -TNF $\alpha$  prevented astrocytic mtFUS-mediated deficits in motor neuron function and survival for a period of time extending to 2 weeks post  $\alpha$ -TNF $\alpha$  administration. While we anticipate that loss of efficacy of the  $\alpha$ -TNF $\alpha$  antibody by our 2-month evaluation timepoint is due to usage and/or diffusion to levels that are sub-threshold to prevent TNF $\alpha$  signaling, we cannot evaluate this directly using our present model. We are able to conclude however, that once the efficacy of  $\alpha$ -TNF $\alpha$  treatment is lost the neurodegenerative process continues to proceed, indicating the mtFUS expression in astrocytes is indeed driving these deleterious consequences.

## 4 | DISCUSSION

Expanding upon our previous *in vitro* work, (Kia et al., 2018; Qosa et al., 2016), in this study we demonstrate that expression of mtFUS in astrocytes alone can drive motor neuron dysfunction and death *in vivo*. Here, we have developed an acute *in vivo* astrocytic expression model in adult mice, using intraspinal AAV injections targeted to spinal levels associated with forelimb motor function. Through this method, we show that astrocytes expressing mtFUS become neurotoxic and induce progressive focal motor neuron dysfunction and death, impairing motor behavior. To our knowledge, this is the first *in vivo* reporting of such astrocytic non-cell autonomous processes in a FUS-ALS model. We also provide evidence that these effects occur through a TNF $\alpha$ -mediated mechanism, identifying an interesting, and potentially mtFUS-specific, toxic pathway to target therapeutically. Indeed, through injection of an  $\alpha$ -TNF $\alpha$  neutralizing antibody we show that it is possible to prevent or block motor neuron degeneration and associated behavioral deficits in mtFUS-expressing animals.

Prior to this work, an astrocyte-specific model of mtFUS expression had not been established, precluding evaluation of astrocyte-based non-cell autonomous effects *in vivo*. The novel model that we have developed demonstrates robust and reproducible behavioral and pathological effects in a brief 2-week time frame. Progression of phenotypes is also observed when comparing effects at 2-weeks versus 2-months. We anticipate that this method may be of considerable utility for others wishing to study astrocyte-mediated effects in neurodegenerative disease where mouse models are otherwise not available, due to rapid behavioral outcome measures and ease of testing therapeutic compounds. However, this system is not ideal for evaluating long-term effects or modeling aspects of FUS-ALS such as disease onset or progression, due to the very targeted and limited expression within the cervical spine region and adult age at which these animals

underwent surgery. As such, while we are curious what the effects of a long-term continuous infusion of  $\alpha$ -TNF $\alpha$  neutralizing antibody via an osmotic pump would be in the background of astrocytic mtFUS expression, we feel that this investigation would be better suited for a chronic mtFUS expression mouse model, rather than the acute system that we have optimized.

Studies at the clinical, genetic, histological, and molecular levels support the hypothesis that neuroinflammation plays a key contributory role in ALS (McCauley & Baloh, 2019). Intriguingly, several previous studies investigating loss of functional FUS protein have suggested that FUS may have a significant role in regulating inflammatory signaling. B-cells derived from FUS-deficient mice have been shown to have reduced responses to traditional B-cell activating stimuli (Hicks et al., 2000). Additionally, FUS-deficient astrocytes display transcriptomic alterations that are enriched for inflammatory genes (Fujioka et al., 2013). Furthermore, while admittedly confined to a small sample size, reduction of FUS levels by 80% in the frontal cortex of marmosets for 6–8 weeks resulted in elevation of both GFAP and Iba1 positive cells and fluorescence intensity, resembling a state of reactive gliosis (Endo et al., 2018). In contrast, overabundance of FUS has also recently been implicated in sensitizing astrocytic and microglial responses to inflammatory environments. Cultured astrocytes overexpressing FUS *in vitro* display enhanced reactivity to inflammatory stimuli, and subsequently cause astrocyte-mediated motor neuron toxicity *in vitro* (Ajmone-Cat et al., 2019). While this complicated picture has emerged where either too little or too much FUS causes a reactive state in astrocytes, it is quite apparent that FUS levels and/or localization are tightly tied to signaling events indicative of cellular distress and inflammation.

At the cellular level, astrocytes act in a multi-faceted way to influence the inflammatory state of the CNS (Colombo & Farina, 2016). In the hippocampus, endogenous basal levels of astroglial-derived TNF $\alpha$  have been shown to be involved in synaptic scaling, whereby TNF $\alpha$  signaling leads to inclusion of calcium permeable GluR1 subunits within amino-3-hydroxy-5-methyl-4-isoxazolepropionic acid (AMPA) receptors in excitatory neurons, as well as decreasing the impact of inhibitory synaptic strength through selective endocytosis of aminobutyric acid type A (GABAA) receptors (Beattie et al., 2002; Santello et al., 2011; Stellwagen et al., 2005; Stellwagen & Malenka, 2006). Alternatively, using a mouse model of multiple sclerosis (experimental autoimmune encephalitis, EAE), where TNF $\alpha$  is elevated above homeostatic levels, it has also been shown that astrocytic TNF $\alpha$  signaling is responsible for N-methyl-D-aspartate (NMDA) receptor-mediated contextual learning/memory impairment (Habbas et al., 2015). Our previous studies investigating the effects of mtFUS astrocytes on wildtype endothelial cells of the blood brain barrier and wildtype spinal cord motor neurons both demonstrated that mutant FUS-expressing astrocytes display changes to genes involved in NF- $\kappa$ B and TNF $\alpha$  signaling pathways (Kia et al., 2018; Qosa et al., 2016), which are known to be potent regulators of inflammatory signaling (Kallioliias & Ivashkiv, 2016). In our *in vitro* co-culture model of mtFUS astrocytes and wildtype motor neurons, we have observed that with highly elevated TNF $\alpha$  levels, motor neuron AMPA receptor subunit



composition is altered in a manner which renders these cells more susceptible to neuronal excitotoxicity (Kia et al., 2018). Further supporting this notion, work by Tolosa et al. has shown that application of exogenous TNF $\alpha$  in the more complex system of organotypic rat spinal cord cultures also evoked glutamate-mediated excitotoxicity, through downregulation of astrocytic excitatory amino acid transporter 2 (EAAT2, also known as glutamate transporter 1 GLT1), elevation of extracellular glutamate levels, and activation of downstream NF- $\kappa$ B pathway oxidative stress responses (Tolosa et al., 2011). In our present work, we similarly demonstrate elevated TNF $\alpha$  mRNA and protein in the spinal cords of mice expressing mtFUS predominantly in astrocytes. We also observe changes to the astrocyte reactivity marker GFAP at the mRNA and protein levels by qRT-PCR and immunohistochemical staining, and by quantification of the number of GFAP immunopositive cells. Additionally, our current work further supports this concept that astrocyte-secreted TNF $\alpha$  is a strong driving factor of motor neuron cell death in FUS-ALS, as expression of mtFUS in animals lacking TNF $\alpha$  did not display evidence of astrocyte reactivity, deficits in motor behavior, or loss of cells in the spinal cord. Furthermore, our evidence suggests that expression of mtFUS in astrocytes is the direct cause of TNF $\alpha$  secretion and activation of gliosis in neighboring cells. If astrogliosis was induced either through our surgical method or by expression of an exogenous protein, we would expect to see increased GFAP<sup>+</sup> cell numbers in TNF $\alpha$  knockout animals as well. Instead, there is no elevation of astrocyte reactivity in these animals, suggesting that it is the TNF $\alpha$  itself that, once released from mtFUS expressing astrocytes, activates other cells in the surround. Finally, our therapeutic intervention strategies targeting soluble TNF $\alpha$  in wildtype (TNF<sup>+/+</sup>) animals also suggest that lowering TNF $\alpha$  in FUS-ALS patients may be beneficial.

Evaluation of TNF $\alpha$  in ALS patients has consistently revealed elevated levels of both membrane bound and soluble TNF $\alpha$  and its receptors. This has been verified in plasma and cerebrospinal fluid (Cereda et al., 2008; Poloni et al., 2000), in post-mortem spinal cords by immunostaining (Kiaei et al., 2006), and in mRNA assessment from post-mortem spinal cord samples (Brambilla et al., 2016). A recent study using next generation RNA sequencing from cervical spinal cord of ALS patients also shows elevation of genes involved in inflammatory processes, with TNF $\alpha$  implicated as the main regulatory molecule for these genes (Brohawn et al., 2016). However, these studies which have examined primarily sporadic ALS patients, have shown that the extent of activation of the NF- $\kappa$ B and TNF $\alpha$  pathways have not correlated with disease duration or severity (Lu et al., 2016; Tateishi et al., 2010). Another layer of complexity also muddies interpretation of TNF $\alpha$ /NF- $\kappa$ B levels from patient samples. In addition to activating downstream signaling cascades, TNF $\alpha$  and NF- $\kappa$ B are known to participate in positive feedback loops where NF- $\kappa$ B can itself regulate TNF $\alpha$  transcription, and TNF signaling can act both in autocrine and paracrine manners to trigger NF- $\kappa$ B activation within an activating cell and in neighboring cells respectively (Gane et al., 2016; Pekalski et al., 2013). Overall, while some of the present evidence does suggest that elevated TNF $\alpha$  levels in ALS are likely a non-specific and self-perpetuating astrocytic and microglial response to degeneration of motor

neurons, other studies have shown that there is a potential correlation between incremental increases in cytokine levels and disease progression (Tortarolo et al., 2017).

A different picture emerges when one focuses more specifically on the genetic forms of ALS. As was previously seen for sporadic cases, NF- $\kappa$ B levels are elevated in both astrocytes and microglia in the mouse model expressing pathogenic mutant superoxide dismutase 1 (SOD1) G93A mutation (Frakes et al., 2014). Further studies in these animals revealed that inhibiting NF- $\kappa$ B solely in astrocytes did not increase motor function or survival, nor did it alter disease progression or onset (Crosio et al., 2011). Preventing NF- $\kappa$ B signaling in microglia however did have a profound effect, preventing motor neuron cell death and extending survival through a mechanism involving reduced release of pro-inflammatory molecules (Frakes et al., 2014). Intriguingly, ablating the TNF $\alpha$  gene completely in SOD1<sup>G93A</sup> or SOD1<sup>G37R</sup> mice did not affect levels of spinal cord astrocytic or microglial reactivity, axon degeneration phenotypes, motor neuron loss, or overall animal survival (Gowing et al., 2006). Therefore, it appears that in the context of SOD1-ALS, that microglia are the major contributing glial population to NF- $\kappa$ B-mediated motor neuron toxicity, but that this effect is due to components of the NF- $\kappa$ B signaling cascade other than TNF $\alpha$ . It is likely therefore, that individuals with SOD1-ALS would not benefit as strongly to TNF $\alpha$  targeting therapeutics. It is not surprising that with different forms of genetic ALS, the mechanisms of non-cell autonomous toxicity may differ, given that different cellular effectors are perturbed as a result of altered protein localization and function. The NF- $\kappa$ B pathway has also been implicated in several models of TDP-43 based ALS, with enhanced NF- $\kappa$ B activation and upregulation of multiple downstream inflammatory cytokines including TNF $\alpha$  (Swarup et al., 2011). In contrast to overall NF- $\kappa$ B pathway upregulation, in both in vitro and in vivo models of mtFUS-ALS, we have now identified and verified TNF $\alpha$ -mediated motor neuron toxicity and suggest that targeting the TNF $\alpha$  may be a particularly promising avenue in genetic patients harboring these mutations (Kia et al., 2018; Qosa et al., 2016).

TNF $\alpha$  exerts its effects on cells through the actions of two ubiquitously expressed surface receptors, termed TNF receptor 1 (TNFR1) and TNF receptor 2 (TNFR2) with TNFR1 preferentially activated by soluble TNF $\alpha$  (sTNF $\alpha$ ) and TNFR2 activated by membrane bound TNF $\alpha$  (mTNF $\alpha$ ) respectively (McCoy & Tansey, 2008). Signaling through these receptors involves differing intracellular cascades and genes involved in either pro- or anti-apoptotic events, as well as pro- or anti-inflammatory signaling. TNF $\alpha$  can therefore alternatively promote protective or toxic effects depending on which receptor is activated. Two recent reviews on this topic are those of Guidotti (Guidotti et al., 2021) and Tortarolo (Tortarolo et al., 2017), which cover the differences in these pathways in much more detail as well as evidence for involvement of these specific receptors in SOD1-ALS mouse models. In our present in vitro and in vivo mtFUS models, we have not yet evaluated the contribution of specific TNF $\alpha$  receptor signaling in the neurotoxic effects that we have seen. The neutralizing antibody that we have utilized targets the signaling portion of the TNF $\alpha$  molecule, so either the mTNF $\alpha$  or secreted sTNF $\alpha$  could be

neutralized following application. Additionally, we have not yet determined which TNFR triggers downstream signaling events. While our present study was focused on identifying TNF $\alpha$  itself as the toxic molecule using a knockout mouse incapable of producing functional TNF $\alpha$  protein, next steps using transgenic animals lacking TNFR1, TNFR2 or both TNFR1/2, will better elucidate the functional pathway of toxicity *in vivo*. On the basis of our *in vitro* work however (Kia et al., 2018), where supernatant from mtFUS astrocytes was toxic when applied to independent wildtype motor neurons in culture, we suspect that sTNF $\alpha$  is the neurotoxic molecule *in vivo* as well, activating TNFR1 and downstream pro-apoptotic cellular cascades. Our ongoing efforts to explicitly target sTNF $\alpha$  or mTNF $\alpha$ , and evaluating cells derived from TNFR receptor knockout animals will shed more light on the cellular mechanisms and downstream pathways involved.

Our results in TNF $\alpha$  knockout animals and effective blocking of motor neuron toxicity through use of an  $\alpha$ -TNF $\alpha$  neutralizing antibody, hint at the potential utility of therapeutically targeting this signaling pathway in FUS-ALS. The testing of TNF $\alpha$  modulating therapeutics in ALS is not a novel concept, and several clinical trials have been run in the past. The first approach was using generic anti-inflammatory agents to inhibit TNF $\alpha$  synthesis. Promising results in SOD1<sup>G93A</sup> mice showed that oral administration of the compound thalidomide improved motor behavior, increased motor neuron survival, delayed disease onset, and slowed disease progression (Kiaei et al., 2006). When TNF $\alpha$  immunoreactivity was examined in the spinal cord, the compound appeared to have the intended effect of destabilizing TNF $\alpha$  mRNA, thus lowering its expression. Unfortunately, when this went to a phase II clinical trial for safety and efficacy in humans, secreted TNF $\alpha$  levels were not impacted, the compound was not well-tolerated at the intended dosing, and disease progression was unaltered (Stommel et al., 2009). Similarly in a Phase III clinical trial, minocycline, which also inhibits TNF $\alpha$  synthesis and improved survival in pre-clinical mouse models, resulted in faster functional deterioration when tested in patients (Gordon et al., 2007). While not yet evaluated for use in ALS patients, an array of anti-TNF $\alpha$  molecules have been recently developed, tested, and approved for inflammatory disorders such as rheumatoid arthritis and Crohn's disease, as well as for the neurodegenerative conditions multiple sclerosis and Alzheimer disease (Sedger & McDermott, 2014). These compounds, such as adalimumab and etanercept, do have serious adverse side-effects, which have been attributed to the non-specificity of action in inhibiting TNF $\alpha$  and general suppression of immune system function (Kemanetzoglou & Andreadou, 2017).

Based on our increasing knowledge of TNF $\alpha$  playing contrasting roles as the pro-inflammatory sTNF $\alpha$  molecule acting on TNFR1, or the anti-inflammatory mTNF $\alpha$  signaling interacting with TNFR2, it is unsurprising that previous clinical trials targeting all TNF $\alpha$  at the translational level or by activity neutralization have yielded underwhelming results and negative immune system ramifications. An exciting new generation compound, XPro1595 selectively targets and neutralizes only sTNF $\alpha$ . In the EAE mouse model of multiple sclerosis, treatment with XPro1595 showed improved remyelination, preservation of axon integrity, and overall clinical outcome, while the non-selective TNF $\alpha$

inhibitor etanercept displayed no recovery of phenotype or function (Brambilla et al., 2011). Similarly, a mouse model of spinal cord injury has also shown that animals receiving XPro1595 demonstrated improved motor function and reduced spinal cord lesion damage, while animals receiving etanercept showed no improvement (Novrup et al., 2014). Importantly, these authors suggest that XPro1595 alters the inflammatory environment by neutralizing sTNF $\alpha$ , without suppressing neuroprotective effects of mTNF $\alpha$  signaling via the TNFR2 receptor (Novrup et al., 2014). Based on these preclinical findings, XPro1595 is eligible for testing in human diseases with known elevation of TNF $\alpha$  levels. In 2019, a Phase 1b trial was begun to assess safety and tolerability in patients with mild to moderate Alzheimer Disease (ClinicalTrials.gov Identifier: NCT03943264).

While further mechanistic investigation into the contributions of astrocytes to neuroinflammation in FUS-ALS are needed, our results do indicate that TNF $\alpha$  signaling leads to motor neuron toxicity *in vivo*. Additionally, our data strengthen the rationale for continued studies of cellular and molecular inflammatory mediators in sporadic ALS, as altered FUS localization or activity may also play a role in driving inflammation in ALS, even when mutated FUS is not the causative mechanism driving the disease (Tyzack et al., 2019). Finally, as medicine progresses towards an era of personalized therapy, it is optimistic to now envision tailored clinical trials to subsets of ALS patients. In our model we have identified TNF $\alpha$  as a promising therapeutic target for FUS-ALS patients. With newer generations of anti-TNF $\alpha$  compounds being generated to target soluble versus membrane TNF $\alpha$  as well as TNFR1 versus TNFR2 receptors, it is our hope that a targeted clinical trial for this subpopulation of genetic ALS patients would ultimately be warranted.

## ACKNOWLEDGMENTS

We would like to acknowledge members of the Jefferson Weinberg ALS Center for suggestions and critical evaluation of this work. We thank laboratory members Kristian Mayer and Thomas Westergard for assistance in preliminary testing of model development and behavioral endpoint testing. N-terminally eGFP tagged human FUS in the pcDNA3.1/nV5-DEST backbone was originally received as a kind gift from Dr. Aaron Gitler. Graphical abstract was created with BioRender.com. This work was supported by funding from the NIH (R01 NS051488 and R01 NS109150 to Piera Pasinelli); the Farber Family Foundation and Family Strong 4 ALS Foundation (to Piera Pasinelli). Brigid K. Jensen was a Family Strong 4 ALS Fellow. Angelo C. Lepore is supported by NIH R01 NS079702 and R01 NS110385. Davide Trotti by RF1-AG057882 and R21-NS0103118 and the Muscular Dystrophy Association, and Aaron R. Haeusler by NIH R00 NS091486 and R21 NS116761 and the Live Like Lou Foundation.

## CONFLICT OF INTEREST

The authors declare no conflicts of interest.

## AUTHOR CONTRIBUTION

Brigid K. Jensen was the lead individual on project conceptualization and visualization, performed experiments, investigation, and analysis,



and wrote the manuscript. Kevin J. McAvoy led initial project conceptualization and visualization, and optimized surgical parameters, time course, and behavioral assessments. Nicolette M. Heinsinger taught the intraspinal surgery technique and performed surgeries on initial cohort of animals for assessment. Angelo C. Lepore developed the intraspinal surgical technique and contributed resources for surgery-related experiments. Hristelina Ilieva, Aaron R. Haeusler, and Davide Trotti were consulted for project visualization, provided supervision, and contributed resources. Piera Pasinelli led project conceptualization, acquired funding, provided supervision and resources, and was the secondary contributor in writing the manuscript. All authors read and approved the final manuscript.

## DATA AVAILABILITY STATEMENT

No large scale data sets have been generated in this study.

## ORCID

Brigid K. Jensen  <https://orcid.org/0000-0003-1624-6307>

Kevin J. McAvoy  <https://orcid.org/0000-0002-0025-1921>

Davide Trotti  <https://orcid.org/0000-0001-6338-6404>

## REFERENCES

- Ajmone-Cat, M. A., Onori, A., Toselli, C., Stronati, E., Morlando, M., Bozzoni, I., Monni, E., Kokaia, Z., Lupo, G., Minghetti, L., Biagioni, S., & Cacci, E. (2019). Increased FUS levels in astrocytes leads to astrocyte and microglia activation and neuronal death. *Scientific Reports*, *9*(1), 4572.
- Averback, P. (1986). A new type of inclusion body in human spinal cord. *Acta Neuropathologica*, *71*(1–2), 106–110.
- Bacskaï, T., Fu, Y., Sengul, G., Ruzsnaç, Z., Paxinos, G., & Watson, C. (2013). Musculotopic organization of the motor neurons supplying forelimb and shoulder girdle muscles in the mouse. *Brain Structure & Function*, *218*(1), 221–238.
- Beattie, E. C., Stellwagen, D., Morishita, W., Bresnahan, J. C., Ha, B. K., Von Zastrow, M., Beattie, M. S., & Malenka, R. C. (2002). Control of synaptic strength by glial TNF $\alpha$ . *Science*, *295*(5563), 2282–2285.
- Brambilla, L., Guidotti, G., Martorana, F., Iyer, A. M., Aronica, E., Valori, C. F., & Rossi, D. (2016). Disruption of the astrocytic TNFR1-GDNF axis accelerates motor neuron degeneration and disease progression in amyotrophic lateral sclerosis. *Human Molecular Genetics*, *25*(14), 3080–3095.
- Brambilla, R., Ashbaugh, J. J., Magliozzi, R., Dellarole, A., Karmally, S., Szymkowski, D. E., & Bethea, J. R. (2011). Inhibition of soluble tumour necrosis factor is therapeutic in experimental autoimmune encephalomyelitis and promotes axon preservation and remyelination. *Brain*, *134*(9), 2736–2754.
- Brohawn, D. G., O'Brien, L. C., & Bennett, J. P., Jr. (2016). RNAseq analyses identify tumor necrosis factor-mediated inflammation as a major abnormality in ALS spinal cord. *PLoS One*, *11*(8), e0160520.
- Bruijn, L. I., Becher, M. W., Lee, M. K., Anderson, K. L., Jenkins, N. A., Copeland, N. G., Sisodia, S. S., Rothstein, J. D., Borchelt, D. R., Price, D. L., & Cleveland, D. W. (1997). ALS-linked SOD1 mutant G85R mediates damage to astrocytes and promotes rapidly progressive disease with SOD1-containing inclusions. *Neuron*, *18*(2), 327–338.
- Cereda, C., Baiocchi, C., Bongioanni, P., Cova, E., Guareschi, S., Metelli, M. R., Rossi, B., Sbalsi, I., Cuccia, M. C., & Ceroni, M. (2008). TNF and sTNFR1/2 plasma levels in ALS patients. *Journal of Neuroimmunology*, *194*(1–2), 123–131.
- Chen, L. (2021). FUS mutation is probably the most common pathogenic gene for JALS, especially sporadic JALS. *Revue Neurologique (Paris)*, *177*(4), 333–340.
- Colombo, E., & Farina, C. (2016). Astrocytes: Key regulators of neuroinflammation. *Trends in Immunology*, *37*(9), 608–620.
- Conlon, E. G., Lu, L., Sharma, A., Yamazaki, T., Tang, T., Shneider, N. A., & Manley, J. L. (2016). The C9ORF72 GGGGCC expansion forms RNA G-quadruplex inclusions and sequesters hnRNP H to disrupt splicing in ALS brains. *eLife*, *5*. <https://doi.org/10.7554/eLife.17820>
- Crosio, C., Valle, C., Casciati, A., Iaccarino, C., & Carri, M. T. (2011). Astroglial inhibition of NF-kappaB does not ameliorate disease onset and progression in a mouse model for amyotrophic lateral sclerosis (ALS). *PLoS One*, *6*(3), e17187.
- Deng, H., Gao, K., & Jankovic, J. (2014). The role of FUS gene variants in neurodegenerative diseases. *Nature Reviews. Neurology*, *10*(6), 337–348.
- Di Giorgio, F. P., Carrasco, M. A., Siao, M. C., Maniatis, T., & Eggan, K. (2007). Non-cell autonomous effect of glia on motor neurons in an embryonic stem cell-based ALS model. *Nature Neuroscience*, *10*(5), 608–614.
- Dokalis, N., & Prinz, M. (2018). Astrocytic NF-kB brings the best and worst out of microglia. *The EMBO Journal*, *37*(16). <https://doi.org/10.15252/embj.2018100130>
- Dormann, D., & Haass, C. (2011). TDP-43 and FUS: A nuclear affair. *Trends in Neurosciences*, *34*(7), 339–348.
- Dormann, D., Madl, T., Valori, C. F., Bentmann, E., Tahirovic, S., Abou-Ajram, C., Kremmer, E., Ansorge, O., Mackenzie, I. R., Neumann, M., & Haass, C. (2012). Arginine methylation next to the PY-NLS modulates transportin binding and nuclear import of FUS. *The EMBO Journal*, *31*(22), 4258–4275.
- Dormann, D., Rodde, R., Edbauer, D., Bentmann, E., Fischer, I., Hruscha, A., Than, M. E., Mackenzie, I. R., Capell, A., Schmid, B., Neumann, M., & Haass, C. (2010). ALS-associated fused in sarcoma (FUS) mutations disrupt transportin-mediated nuclear import. *The EMBO Journal*, *29*(16), 2841–2857.
- Endo, K., Ishigaki, S., Masamizu, Y., Fujioka, Y., Watakabe, A., Yamamori, T., Hatanaka, N., Nambu, A., Okado, H., Katsuno, M., Watanabe, H., Matsuzaki, M., & Sobue, G. (2018). Silencing of FUS in the common marmoset (*Callithrix jacchus*) brain via stereotaxic injection of an adeno-associated virus encoding shRNA. *Neuroscience Research*, *130*, 56–64.
- Ferrer, I., Legati, A., Garcia-Monco, J. C., Gomez-Beldarrain, M., Carmona, M., Blanco, R., Seeley, W. W., & Coppola, G. (2015). Familial behavioral variant frontotemporal dementia associated with astrocyte-predominant tauopathy. *Journal of Neuropathology and Experimental Neurology*, *74*(4), 370–379.
- Filipi, T., Hermanova, Z., Tureckova, J., Vanatko, O., & Anderova, M. (2020). Glial cells—the strategic targets in amyotrophic lateral sclerosis treatment. *Journal of Clinical Medicine*, *9*(1), 261. <https://doi.org/10.3390/jcm9010261>
- Finsterbusch, M., Hall, P., Li, A., Devi, S., Westhorpe, C. L., Kitching, A. R., & Hickey, M. J. (2016). Patrolling monocytes promote intravascular neutrophil activation and glomerular injury in the acutely inflamed glomerulus. *Proceedings of the National Academy of Sciences of the United States of America*, *113*(35), 5172–5181.
- Frakes, A. E., Ferraiuolo, L., Haidet-Phillips, A. M., Schmelzer, L., Braun, L., Miranda, C. J., Ladner, K. J., Bevan, A. K., Foust, K. D., Godbout, J. P., Popovich, P. G., Guttridge, D. C., & Kaspar, B. K. (2014). Microglia induce motor neuron death via the classical NF-kappaB pathway in amyotrophic lateral sclerosis. *Neuron*, *81*(5), 1009–1023.
- Fujimori, K., Ishikawa, M., Otomo, A., Atsuta, N., Nakamura, R., Akiyama, T., Hadano, S., Aoki, M., Saya, H., Sobue, G., & Okano, H. (2018). Modeling sporadic ALS in iPSC-derived motor neurons identifies a potential therapeutic agent. *Nature Medicine*, *24*(10), 1579–1589.

- Fujioka, Y., Ishigaki, S., Masuda, A., Iguchi, Y., Udagawa, T., Watanabe, H., Katsuno, M., Ohno, K., & Sobue, G. (2013). FUS-regulated region- and cell-type-specific transcriptome is associated with cell selectivity in ALS/FTLD. *Scientific Reports*, 3, 2388.
- Gandelman, M., Peluffo, H., Beckman, J. S., Cassina, P., & Barbeito, L. (2010). Extracellular ATP and the P2X7 receptor in astrocyte-mediated motor neuron death: Implications for amyotrophic lateral sclerosis. *Journal of Neuroinflammation*, 7, 33.
- Gane, J. M., Stockley, R. A., & Sapey, E. (2016). TNF-alpha autocrine feedback loops in human monocytes: The pro- and anti-inflammatory roles of the TNF-alpha receptors support the concept of selective TNFR1 blockade in vivo. *Journal of Immunology Research*, 2016, 1079851.
- Gong, Y. H., Parsadanian, A. S., Andreeva, A., Snider, W. D., & Elliott, J. L. (2000). Restricted expression of G86R cu/Zn superoxide dismutase in astrocytes results in astrocytosis but does not cause motoneuron degeneration. *The Journal of Neuroscience*, 20(2), 660-665.
- Gordon, P. H., Moore, D. H., Miller, R. G., Florence, J. M., Verheijde, J. L., Doorish, C., Hilton, J. F., Spitalny, G. M., MacArthur, R. B., Mitsumoto, H., Neville, H. E., Boylan, K., Mozaffar, T., Belsh, J. M., Ravits, J., Bedlack, R. S., Graves, M. C., McCluskey, L. F., Barohn, R. J., & Western, A. L. S. S. G. (2007). Efficacy of minocycline in patients with amyotrophic lateral sclerosis: A phase III randomised trial. *Lancet Neurology*, 6(12), 1045-1053.
- Gowing, G., Dequen, F., Soucy, G., & Julien, J. P. (2006). Absence of tumor necrosis factor-alpha does not affect motor neuron disease caused by superoxide dismutase 1 mutations. *The Journal of Neuroscience*, 26(44), 11397-11402.
- Guidotti, G., Scarlata, C., Brambilla, L., & Rossi, D. (2021). Tumor necrosis factor alpha in amyotrophic lateral sclerosis: Friend or foe? *Cells*, 10(3), 518-537. <https://doi.org/10.3390/cells10030518>
- Habbas, S., Santello, M., Becker, D., Stubbe, H., Zappia, G., Liadet, N., Klaus, F. R., Kollias, G., Fontana, A., Pryce, C. R., Suter, T., & Volterra, A. (2015). Neuroinflammatory TNFalpha impairs memory via astrocyte signaling. *Cell*, 163(7), 1730-1741.
- Hensley, K., Fedynyshyn, J., Ferrell, S., Floyd, R. A., Gordon, B., Grammas, P., Hamdheydari, L., Mhatre, M., Mou, S., Pye, Q. N., Stewart, C., West, M., West, S., & Williamson, K. S. (2003). Message and protein-level elevation of tumor necrosis factor alpha (TNF alpha) and TNF alpha-modulating cytokines in spinal cords of the G93A-SOD1 mouse model for amyotrophic lateral sclerosis. *Neurobiology of Disease*, 14(1), 74-80.
- Hewitt, C., Kirby, J., Highley, J. R., Hartley, J. A., Hibberd, R., Hollinger, H. C., Williams, T. L., Ince, P. G., McDermott, C. J., & Shaw, P. J. (2010). Novel FUS/TLS mutations and pathology in familial and sporadic amyotrophic lateral sclerosis. *Archives of Neurology*, 67(4), 455-461.
- Hicks, G. G., Singh, N., Nashabi, A., Mai, S., Bozek, G., Klewes, L., Arapovic, D., White, E. K., Koury, M. J., Oltz, E. M., Van Kaer, L., & Ruley, H. E. (2000). Fus deficiency in mice results in defective B-lymphocyte development and activation, high levels of chromosomal instability and perinatal death. *Nature Genetics*, 24(2), 175-179.
- Ikenaka, K., Ishigaki, S., Iguchi, Y., Kawai, K., Fujioka, Y., Yokoi, S., Abdelhamid, R. F., Nagano, S., Mochizuki, H., Katsuno, M., & Sobue, G. (2020). Characteristic features of FUS inclusions in spinal motor neurons of sporadic amyotrophic lateral sclerosis. *Journal of Neuropathology and Experimental Neurology*, 79(4), 370-377.
- Kallioulas, G. D., & Ivashkiv, L. B. (2016). TNF biology, pathogenic mechanisms and emerging therapeutic strategies. *Nature Reviews Rheumatology*, 12(1), 49-62.
- Kamo, H., Haebara, H., Akiguchi, I., Kameyama, M., Kimura, H., & McGeer, P. L. (1987). A distinctive distribution of reactive astroglia in the precentral cortex in amyotrophic lateral sclerosis. *Acta Neuropathologica*, 74(1), 33-38.
- Kemanetzoglou, E., & Andreadou, E. (2017). CNS demyelination with TNF-alpha blockers. *Current Neurology and Neuroscience Reports*, 17(4), 36.
- Kia, A., McAvoy, K., Krishnamurthy, K., Trotti, D., & Pasinelli, P. (2018). Astrocytes expressing ALS-linked mutant FUS induce motor neuron death through release of tumor necrosis factor-alpha. *GLIA*, 66(5), 1016-1033.
- Kiaei, M., Petri, S., Kipiani, K., Gardian, G., Choi, D. K., Chen, J., Calingasan, N. Y., Schafer, P., Muller, G. W., Stewart, C., Hensley, K., & Beal, M. F. (2006). Thalidomide and lenalidomide extend survival in a transgenic mouse model of amyotrophic lateral sclerosis. *The Journal of Neuroscience*, 26(9), 2467-2473.
- Kimura, T., & Budka, H. (1984). Glial bundles in spinal nerve roots. An immunocytochemical study stressing their nonspecificity in various spinal cord and peripheral nerve diseases. *Acta Neuropathologica*, 65(1), 46-52.
- Kobayashi, Z., Tsuchiya, K., Arai, T., Aoki, M., Hasegawa, M., Ishizu, H., Akiyama, H., & Mizusawa, H. (2010). Occurrence of basophilic inclusions and FUS-immunoreactive neuronal and glial inclusions in a case of familial amyotrophic lateral sclerosis. *Journal of the Neurological Sciences*, 293(1-2), 6-11.
- Kushner, P. D., Stephenson, D. T., & Wright, S. (1991). Reactive astrogliosis is widespread in the subcortical white matter of amyotrophic lateral sclerosis brain. *Journal of Neuropathology and Experimental Neurology*, 50(3), 263-277.
- Kwiatkowski, T. J., Jr., Bosco, D. A., Leclerc, A. L., Tamrazian, E., Vanderburg, C. R., Russ, C., Davis, A., Gilchrist, J., Kasarskis, E. J., Munsat, T., Valdmanis, P., Rouleau, G. A., Hosler, B. A., Cortelli, P., de Jong, P. J., Yoshinaga, Y., Haines, J. L., Pericak-Vance, M. A., Yan, J., & Brown, R. H., Jr. (2009). Mutations in the FUS/TLS gene on chromosome 16 cause familial amyotrophic lateral sclerosis. *Science*, 323(5918), 1205-1208.
- Li, K., Hala, T. J., Seetharam, S., Poulsen, D. J., Wright, M. C., & Lepore, A. C. (2015). GLT1 overexpression in SOD1(G93A) mouse cervical spinal cord does not preserve diaphragm function or extend disease. *Neurobiology of Disease*, 78, 12-23.
- Li, K., Nicaise, C., Sannie, D., Hala, T. J., Javed, E., Parker, J. L., Putatunda, R., Regan, K. A., Suain, V., Brion, J. P., Rhoderick, F., Wright, M. C., Poulsen, D. J., & Lepore, A. C. (2014). Overexpression of the astrocyte glutamate transporter GLT1 exacerbates phrenic motor neuron degeneration, diaphragm compromise, and forelimb motor dysfunction following cervical contusion spinal cord injury. *The Journal of Neuroscience*, 34(22), 7622-7638.
- Lu, C. H., Allen, K., Oei, F., Leoni, E., Kuhle, J., Tree, T., Fratta, P., Sharma, N., Sidle, K., Howard, R., Orrell, R., Fish, M., Greensmith, L., Pearce, N., Gallo, V., & Malaspina, A. (2016). Systemic inflammatory response and neuromuscular involvement in amyotrophic lateral sclerosis. *Neurology Neuroimmunology & Neuroinflammation*, 3(4), e244.
- Machamer, J. B., Collins, S. E., & Lloyd, T. E. (2014). The ALS gene FUS regulates synaptic transmission at the drosophila neuromuscular junction. *Human Molecular Genetics*, 23(14), 3810-3822.
- McCaughey, M. E., & Baloh, R. H. (2019). Inflammation in ALS/FTD pathogenesis. *Acta Neuropathologica*, 137(5), 715-730.
- McCoy, M. K., & Tansey, M. G. (2008). TNF signaling inhibition in the CNS: Implications for normal brain function and neurodegenerative disease. *Journal of Neuroinflammation*, 5, 45.
- Meyer, K., Ferraiuolo, L., Miranda, C. J., Likhite, S., McElroy, S., Rensch, S., Ditsworth, D., Lagier-Tourenne, C., Smith, R. A., Ravits, J., Burghes, A. H., Shaw, P. J., Cleveland, D. W., Kolb, S. J., & Kaspar, B. K. (2014). Direct conversion of patient fibroblasts demonstrates non-cell autonomous toxicity of astrocytes to motor neurons in familial and sporadic ALS. *Proceedings of the National Academy of Sciences of the United States of America*, 111(2), 829-832.
- Migheli, A., Piva, R., Atzori, C., Troost, D., & Schiffer, D. (1997). C-Jun, JNK/SAPK kinases and transcription factor NF-kappa B are selectively activated in astrocytes, but not motor neurons, in amyotrophic lateral sclerosis. *Journal of Neuropathology and Experimental Neurology*, 56(12), 1314-1322.



- Mizielinska, S., Lashley, T., Norona, F. E., Clayton, E. L., Ridler, C. E., Fratta, P., & Isaacs, A. M. (2013). C9orf72 frontotemporal lobar degeneration is characterised by frequent neuronal sense and antisense RNA foci. *Acta Neuropathologica*, 126(6), 845–857.
- Mulder, D. W. (1982). Clinical limits of amyotrophic lateral sclerosis. *Advances in Neurology*, 36, 15–22.
- Murayama, S., Inoue, K., Kawakami, H., Bouldin, T. W., & Suzuki, K. (1991). A unique pattern of astrocytosis in the primary motor area in amyotrophic lateral sclerosis. *Acta Neuropathologica*, 82(6), 456–461.
- Nagai, M., Re, D. B., Nagata, T., Chalazonitis, A., Jessell, T. M., Wichterle, H., & Przedborski, S. (2007). Astrocytes expressing ALS-linked mutated SOD1 release factors selectively toxic to motor neurons. *Nature Neuroscience*, 10(5), 615–622.
- Nagy, D., Kato, T., & Kushner, P. D. (1994). Reactive astrocytes are widespread in the cortical gray matter of amyotrophic lateral sclerosis. *Journal of Neuroscience Research*, 38(3), 336–347.
- Novrup, H. G., Bracchi-Ricard, V., Ellman, D. G., Ricard, J., Jain, A., Runko, E., Lyck, L., Yli-Karjanmaa, M., Szymkowski, D. E., Pearse, D. D., Lambertsen, K. L., & Bethea, J. R. (2014). Central but not systemic administration of XPro1595 is therapeutic following moderate spinal cord injury in mice. *Journal of Neuroinflammation*, 11, 159.
- Pasparakis, M., Alexopoulou, L., Episkopou, V., & Kollias, G. (1996). Immune and inflammatory responses in TNF alpha-deficient mice: A critical requirement for TNF alpha in the formation of primary B cell follicles, follicular dendritic cell networks and germinal centers, and in the maturation of the humoral immune response. *The Journal of Experimental Medicine*, 184(4), 1397–1411.
- Pekalski, J., Zuk, P. J., Kochanczyk, M., Junkin, M., Kellogg, R., Tay, S., & Lipniacki, T. (2013). Spontaneous NF-kappaB activation by autocrine TNFalpha signaling: A computational analysis. *PLoS One*, 8(11), e78887.
- Phatnani, H. P., Guarnieri, P., Friedman, B. A., Carrasco, M. A., Muratet, M., O'Keefe, S., Nwakeze, C., Pauli-Behn, F., Newberry, K. M., Meadows, S. K., Tapia, J. C., Myers, R. M., & Maniatis, T. (2013). Intricate interplay between astrocytes and motor neurons in ALS. *Proceedings of the National Academy of Sciences of the United States of America*, 110(8), 756–765.
- Poloni, M., Facchetti, D., Mai, R., Micheli, A., Agnoletti, L., Francolini, G., Mora, G., Camana, C., Mazzini, L., & Bachetti, T. (2000). Circulating levels of tumour necrosis factor-alpha and its soluble receptors are increased in the blood of patients with amyotrophic lateral sclerosis. *Neuroscience Letters*, 287(3), 211–214.
- Popova, L. M., & Sakharova, A. V. (1982). Virus-like inclusions in the cells of the central nervous system in amyotrophic lateral sclerosis. *Arkhiv Patologii*, 44(10), 28–33.
- Qian, K., Huang, H., Peterson, A., Hu, B., Maragakis, N. J., Ming, G. L., Chen, H., & Zhang, S. C. (2017). Sporadic ALS astrocytes induce neuronal degeneration in vivo. *Stem Cell Reports*, 8(4), 843–855.
- Qosa, H., Lichter, J., Sarlo, M., Markandaiah, S. S., McAvoy, K., Richard, J. P., Jablonski, M. R., Maragakis, N. J., Pasinelli, P., & Trotti, D. (2016). Astrocytes drive upregulation of the multidrug resistance transporter ABCB1 (P-glycoprotein) in endothelial cells of the blood-brain barrier in mutant superoxide dismutase 1-linked amyotrophic lateral sclerosis. *GLIA*, 64(8), 1298–1313.
- Rademakers, R., Stewart, H., DeJesus-Hernandez, M., Krieger, C., Graff-Radford, N., Fabros, M., Briemberg, H., Cashman, N., Eisen, A., & Mackenzie, I. R. (2010). Fus gene mutations in familial and sporadic amyotrophic lateral sclerosis. *Muscle & Nerve*, 42(2), 170–176.
- Renton, A. E., Chio, A., & Traynor, B. J. (2014). State of play in amyotrophic lateral sclerosis genetics. *Nature Neuroscience*, 17(1), 17–23.
- Rostalski, H., Leskela, S., Huber, N., Katisko, K., Cajanus, A., Solje, E., Marttinen, M., Natunen, T., Remes, A. M., Hiltunen, M., & Haapasalo, A. (2019). Astrocytes and microglia as potential contributors to the pathogenesis of C9orf72 repeat expansion-associated FTL and ALS. *Frontiers in Neuroscience*, 13, 486.
- Santello, M., Bezzi, P., & Volterra, A. (2011). TNFalpha controls glutamatergic gliotransmission in the hippocampal dentate gyrus. *Neuron*, 69(5), 988–1001.
- Scekic-Zahirovic, J., Oussini, H. E., Mersmann, S., Drenner, K., Wagner, M., Sun, Y., Allmeroth, K., Dieterle, S., Sinniger, J., Dirrig-Grosch, S., Rene, F., Dormann, D., Haass, C., Ludolph, A. C., Lagier-Tourenne, C., Storkebaum, E., & Dupuis, L. (2017). Motor neuron intrinsic and extrinsic mechanisms contribute to the pathogenesis of FUS-associated amyotrophic lateral sclerosis. *Acta Neuropathologica*, 133(6), 887–906.
- Sedger, L. M., & McDermott, M. F. (2014). TNF and TNF-receptors: From mediators of cell death and inflammation to therapeutic giants - past, present and future. *Cytokine & Growth Factor Reviews*, 25(4), 453–472.
- Sharma, A., Lyashchenko, A. K., Lu, L., Nasrabad, S. E., Elmaleh, M., Mendelsohn, M., Nemes, A., Tapia, J. C., Mentis, G. Z., & Shneider, N. A. (2016). ALS-associated mutant FUS induces selective motor neuron degeneration through toxic gain of function. *Nature Communications*, 7, 10465.
- Stellwagen, D., Beattie, E. C., Seo, J. Y., & Malenka, R. C. (2005). Differential regulation of AMPA receptor and GABA receptor trafficking by tumor necrosis factor-alpha. *The Journal of Neuroscience*, 25(12), 3219–3228.
- Stellwagen, D., & Malenka, R. C. (2006). Synaptic scaling mediated by glial TNF-alpha. *Nature*, 440(7087), 1054–1059.
- Stommel, E. W., Cohen, J. A., Fadul, C. E., Cogbill, C. H., Graber, D. J., Kingman, L., Mackenzie, T., Channon Smith, J. Y., & Harris, B. T. (2009). Efficacy of thalidomide for the treatment of amyotrophic lateral sclerosis: A phase II open label clinical trial. *Amyotrophic Lateral Sclerosis*, 10(5–6), 393–404.
- Strong, M. J., Abrahams, S., Goldstein, L. H., Woolley, S., McLaughlin, P., Snowden, J., Mioshi, E., Roberts-South, A., Benatar, M., HortobaGyi, T., Rosenfeld, J., Silani, V., Ince, P. G., & Turner, M. R. (2017). Amyotrophic lateral sclerosis - frontotemporal spectrum disorder (ALS-FTSD): Revised diagnostic criteria. *Amyotrophic Lateral Sclerosis and Frontotemporal Degeneration*, 18(3–4), 153–174.
- Suzuki, N., Kato, S., Kato, M., Warita, H., Mizuno, H., Kato, M., Shimakura, N., Akiyama, H., Kobayashi, Z., Konno, H., & Aoki, M. (2012). FUS/TLS-immunoreactive neuronal and glial cell inclusions increase with disease duration in familial amyotrophic lateral sclerosis with an R521C FUS/TLS mutation. *Journal of Neuropathology and Experimental Neurology*, 71(9), 779–788.
- Swarup, V., Phaneuf, D., Dupre, N., Petri, S., Strong, M., Kriz, J., & Julien, J. P. (2011). Deregulation of TDP-43 in amyotrophic lateral sclerosis triggers nuclear factor kappaB-mediated pathogenic pathways. *The Journal of Experimental Medicine*, 208(12), 2429–2447.
- Tateishi, T., Yamasaki, R., Tanaka, M., Matsushita, T., Kikuchi, H., Isobe, N., Ohyagi, Y., & Kira, J. (2010). CSF chemokine alterations related to the clinical course of amyotrophic lateral sclerosis. *Journal of Neuroimmunology*, 222(1–2), 76–81.
- Tolosa, L., Caraballo-Miralles, V., Olmos, G., & Llado, J. (2011). TNF-alpha potentiates glutamate-induced spinal cord motoneuron death via NF-kappaB. *Molecular and Cellular Neurosciences*, 46(1), 176–186.
- Tong, J., Huang, C., Bi, F., Wu, Q., Huang, B., Liu, X., Li, F., Zhou, H., & Xia, X. G. (2013). Expression of ALS-linked TDP-43 mutant in astrocytes causes non-cell-autonomous motor neuron death in rats. *The EMBO Journal*, 32(13), 1917–1926.
- Tortarolo, M., Lo Coco, D., Veglianesi, P., Vallarola, A., Giordana, M. T., Marcon, G., Beghi, E., Poloni, M., Strong, M. J., Iyer, A. M., Aronica, E., & Bendotti, C. (2017). Amyotrophic lateral sclerosis, a multisystem pathology: Insights into the role of TNFalpha. *Mediators of Inflammation*, 2017, 2985051.
- Tripathi, P., Rodriguez-Muela, N., Klim, J. R., de Boer, A. S., Agrawal, S., Sandoe, J., Lopes, C. S., Oglari, K. S., Williams, L. A., Shear, M., Rubin, L. L., Eggan, K., & Zhou, Q. (2017). Reactive astrocytes promote ALS-like degeneration and intracellular protein aggregation in human

- motor neurons by disrupting autophagy through TGF-beta1. *Stem Cell Reports*, 9(2), 667–680.
- Tyzack, G. E., Hall, C. E., Sibley, C. R., Cymes, T., Forostyak, S., Carlino, G., Meyer, I. F., Schiavo, G., Zhang, S. C., Gibbons, G. M., Newcombe, J., Patani, R., & Lakatos, A. (2017). A neuroprotective astrocyte state is induced by neuronal signal EphB1 but fails in ALS models. *Nature Communications*, 8(1), 1164.
- Tyzack, G. E., Luisier, R., Taha, D. M., Neeves, J., Modic, M., Mitchell, J. S., Meyer, I., Greensmith, L., Newcombe, J., Ule, J., Luscombe, N. M., & Patani, R. (2019). Widespread FUS mislocalization is a molecular hallmark of amyotrophic lateral sclerosis. *Brain*, 142(9), 2572–2580.
- Valori, C. F., Brambilla, L., Martorana, F., & Rossi, D. (2014). The multifaceted role of glial cells in amyotrophic lateral sclerosis. *Cellular and Molecular Life Sciences*, 71(2), 287–297.
- Vance, C., Rogelj, B., Hortobagyi, T., De Vos, K. J., Nishimura, A. L., Sreedharan, J., Hu, X., Smith, B., Ruddy, D., Wright, P., Ganesalingam, J., Williams, K. L., Tripathi, V., Al-Saraj, S., Al-Chalabi, A., Leigh, P. N., Blair, I. P., Nicholson, G., de Bellerocche, J., & Shaw, C. E. (2009). Mutations in FUS, an RNA processing protein, cause familial amyotrophic lateral sclerosis type 6. *Science*, 323(5918), 1208–1211.
- Vance, C., Scotter, E. L., Nishimura, A. L., Troakes, C., Mitchell, J. C., Kathe, C., Urwin, H., Manser, C., Miller, C. C., Hortobagyi, T., Dragunow, M., Rogelj, B., & Shaw, C. E. (2013). ALS mutant FUS disrupts nuclear localization and sequesters wild-type FUS within cytoplasmic stress granules. *Human Molecular Genetics*, 22(13), 2676–2688.
- Via, C. S., Shustov, A., Rus, V., Lang, T., Nguyen, P., & Finkelman, F. D. (2001). In vivo neutralization of TNF-alpha promotes humoral autoimmunity by preventing the induction of CTL. *Journal of Immunology*, 167(12), 6821–6826.
- Vucic, S., Rothstein, J. D., & Kiernan, M. C. (2014). Advances in treating amyotrophic lateral sclerosis: Insights from pathophysiological studies. *Trends in Neurosciences*, 37(8), 433–442.
- Wachter, N., Storch, A., & Hermann, A. (2015). Human TDP-43 and FUS selectively affect motor neuron maturation and survival in a murine cell model of ALS by non-cell-autonomous mechanisms. *Amyotrophic Lateral Sclerosis and Frontotemporal Degeneration*, 16(7–8), 431–441.
- Wang, R., Yang, B., & Zhang, D. (2011). Activation of interferon signaling pathways in spinal cord astrocytes from an ALS mouse model. *GLIA*, 59(6), 946–958.
- Zou, Z. Y., Liu, M. S., Li, X. G., & Cui, L. Y. (2016). Mutations in FUS are the most frequent genetic cause in juvenile sporadic ALS patients of Chinese origin. *Amyotrophic Lateral Sclerosis and Frontotemporal Degeneration*, 17(3–4), 249–252.
- Zou, Z. Y., Zhou, Z. R., Che, C. H., Liu, C. Y., He, R. L., & Huang, H. P. (2017). Genetic epidemiology of amyotrophic lateral sclerosis: A systematic review and meta-analysis. *Journal of Neurology, Neurosurgery, and Psychiatry*, 88(7), 540–549.

## SUPPORTING INFORMATION

Additional supporting information may be found in the online version of the article at the publisher's website.

**How to cite this article:** Jensen, B. K., McAvoy, K. J., Heinsinger, N. M., Lepore, A. C., Ilieva, H., Haeusler, A. R., Trotti, D., & Pasinelli, P. (2022). Targeting TNF $\alpha$  produced by astrocytes expressing amyotrophic lateral sclerosis-linked mutant fused in sarcoma prevents neurodegeneration and motor dysfunction in mice. *Glia*, 70(7), 1426–1449. <https://doi.org/10.1002/glia.24183>